Heliyon 7 (2021) e08569

Contents lists available at ScienceDirect

Heliyon

journal homepage: www.cell.com/heliyon

Research article

Vegetation climate and marine environmental reconstruction in the western Mediterranean (southern Rifian corridor, Morocco) over the Tortonian-Messinian transition

Soukaina Targhi [a,*], Nadia Barhoun [a], Naima Bachiri Taoufiq [a], Mohamed Achab [b], Abdallah Ait Salem [c], Mohamed Zakaria Yousfi [c]

[a] Hassan II University of Casablanca, Faculty of Sciences Ben M'sik, Geology Department, Geosciences and Applications Laboratory, B.P 7955, Sidi Othmane Casablanca, Morocco
[b] Scientific Institute, University Mohammed V in Rabat, Avenue Ibn Batouta, P.B. 703, 10106 Rabat-Agdal, Morocco
[c] National Office of Hydrocarbons and Mines (ONHYM) Rabat, Morocco

ARTICLE INFO

Keywords:
Climate
Vegetation
Marine environment
Western Mediterranean
South Rifian corridor
Tortonian-Messinian transition

ABSTRACT

The Southern Rifian Corridor was a gateway connecting the Mediterranean Sea to the Atlantic Ocean in the Late Miocene. Its rapid narrowing at the Tortonian - Messinian transition around 7.2 Ma, resulting from very intense tectonic activity, has triggered an ecological crisis well before the deposition of the Messinian Salinity crisis evaporites.

The sedimentary successions deposited in the Saïs Basin have recorded different events regarding biostratigraphic, environmental, tectonic, and eustatic that characterized the area during the late Miocene. In order to get information on the marine and continental environment during the Tortonian-Messinian Transition (TMT), a palynological and biostratigraphic study was carried out on two boreholes in the Saïs Basin.

The biostratigraphic analyses based on the planktonic foraminifera of the boreholes studied reveals the succession of several biostratigraphic events, allowing us to attribute these sedimentary deposits to the late Tortonian - early Messinian time interval including the recognition of the T/M boundary.

The abundance of continental inputs (pollen, spores, BOM, WOM, and COM in the palynofacies) and the low D/S ratio values indicated that the Saïs basin was a neritic epicontinental environment suffering a significant influence of terrigenous inputs. The temperature index shows that the thermal conditions of the surface water were warm.

In the late Tortonian, faunal and floristic assemblages indicate an open, relatively deep, outer platform type marine environment with a slight tendency towards an inner platform context. At the Tortonian-Messinian boundary, there is an increase in land inputs and relative reduction in the diversity of both microfauna and microflora. The presence of cold-water taxa probably indicates moderate cooling. In Lower Messinian the marine environment, was external platform with tendencies towards an internal area.

The cover is opened and dominated by herbaceous plants that colonize the low altitudes, while trees colonized the middle altitudes. The climate was hot and humid in the mid-altitude and dry in the lowlands.

1. Introduction

In the late Miocene, the Mediterranean basin registers an extreme geological event known as the "Messinian salinity crisis" (MSC, 5.97–5.33 Ma) (Hsü et al., 1973). This event was the result of a gradual closure of ancient connections linking the Mediterranean and the Atlantic Ocean in Gibraltar region. As a result, impressive evaporitic masses (mainly gypsum and halite) exceed 1 million km3 have been accumulated, forming locally more than 2 km thick of salt layers in the center of the Mediterranean (Hsü et al., 1973, CIESM, 2008; Roveri et al., 2014; Karakitsios et al., 2017a,b; Suc, 1996, 2019). This unusual geological event has caused rapid and major palaeoenvironmental variations in the Mediterranean basin (Vasiliev et al., 2013, 2019; Roveri et al., 2014; Flecker et al., 2015; Agiadi et al., 2017; Karakitsios et al., 2017b;

* Corresponding author.
E-mail address: targhi.sokaina@gmail.com (S. Targhi).

https://doi.org/10.1016/j.heliyon.2021.e08569
Received 8 April 2021; Received in revised form 7 July 2021; Accepted 3 December 2021

Moissette et al., 2018; Suc and Frizon de Lamotte, 2019; Kontakiotis et al., 2019, 2020 a,b).

The Southern Rifian Corridor, together with the Betic Corridors, represents key elements required to understand exchanges between the Atlantic and the Mediterranean at the end of the Miocene. The Miocene and Pliocene sedimentary successions deposited inside this Corridor have recorded all the various biostratigraphical, environmental, tectonic and eustatic events that preceded the MSC (Barhoun et al., 2008; Capella et al., 2018b; Flecker et al., 2015; Achalhi et al., 2016; Azdimousa et al., 2011). Thus, the sediments exposed in all of this corridor have been extensively studied in order to understand the complex evolution of the different corridors linking the Mediterranean and the Atlantic Ocean as well as the succession of hydrological events that led to that giant saliferous formation (Krijgsman et al., 1999a, 2018; Manzi et al., 2013; Capella et al., 2017a; b).

The previous research indicates that water exchanges between the Mediterranean Sea and the Atlantic Ocean have persisted during the interval 6.7 Ma - 5.55 Ma (Krijgsman et al., 1999b; Flecker et al., 2015; Simon and Meijer, 2015; Achalhi et al., 2016), allowing the accumulation of thick saliferous series in the Mediterranean sea (Cornée et al., 2006; Krijgsman and Meijer, 2008; Topper et al., 2011; Meijer, 2012; Topper and Meijer, 2013, 2015; Simon and Meijer, 2015; Tulbure et al., 2017; Vasiliev et al., 2019; Kontakiotis et al., 2019).

After the closing of the Betic Corridors at 7.2 Ma (Martin et al., 2014; Flecker et al., 2015; Krijgsman et al., 2018), the Rifian Corridor becomes the most important marine way connecting the Mediterranean with the Atlantic. It was the last connection before the MSC and closed at 7.1–6.9 Ma, in its southern branch and at 7.35–7.25 Ma, in its northern branch (Flecker et al., 2015; Capella et al., 2018b; Krijgsman et al., 2018).

Although geological studies on this topic are abundant, the chronology of corridor opening and closing, changes in palaeoenvironmental parameters and palaeoclimatic reconstructions are still subject to several discussions (Krijgsman et al., 1999a; Achalhi et al., 2016; Capella et al., 2017a).

The change in the geometry of the Mediterranean-Atlantic connecting gateway can significantly modify both the global ocean circulation and the associated climate while also having a profound impact in regional environmental change (Flecker et al., 2015; Karakitsios et al., 2017a; Krijgsman et al. et al., 2018; Vasiliev et al., 2019). The understanding of the hydrographic changes and their link to climate and/or tectonics that led to the Messinian salinity crisis is however still debated.

In addition, the consequences of corridor narrowing and water impoverishment on faunal and floral communities are insufficiently studied and poorly known, especially at the TMT (Moissette et al., 2018).

In order to contribute to understanding the consequences of the southern Rifian corridor narrowing and water impoverishment on the microfauna and microflora during the late Miocene and in particular, at the TMT, we conducted an integrated biostratigraphic and palynological study of the late Miocene in the Saïs Basin (western Rifian corridor). This study will allow to reconstruct evolution of vegetation, climate and marine environment during the TMT in precise chronostratigraphic framework.

Through the detailed study of the associations of planktonic foraminifera, the ecological analyses of marine microfossils (planktonic foraminifera and dinocysts), completed by the study of terrestrial palynomorphs (pollen grains, spores...), our work will focus on a triple objective. The first objective is to establish a precise biostratigraphic framework of the Miocene sediments of the Saïs basin. The second objective is contributes to reconstruct the paleoenvironment and sea surface conditions and thus to characterize the paleoceanographic evolution communications between the Atlantic and the Mediterranean through the southern Rifian corridor during the late Miocene. The third objective is to trace the evolution of vegetation and climate during the Tortonian-Messinian period from pollen grain.

2. Geographical and geological setting

Due to its particular position in the south Rifian corridor, Saïs basin has been subjected to diverse geological studies such as those of Talatasse (1953); Margat and Talatasse (1954); Choubert and Fauve Muret (1962); Feinberg Lorenz (1970); Martin (1977); Feinberg (1978); Ait Brahim (1983); Cirac (1987); Wernli (1988); Kili (1993); Zizi (1996); Ben Moussa et al. (1997); Fassi (1999); Chalouan et al. (2014); Flecker et al. (2015); Tulbure et al. (2017); Capella et al. (2017a, b); Capella et al. (2018a,b).

The Saïs basin is a depression elongated from east to west for about 110 km in length and 30 km in width. It is limited by: The South rifian Ridges and the Prerif domain in the north, the Meseto-Atlasic domain in the south, the Beht valley and El Kansra sill in the west and the Tazekka reliefs and Taza sill in the east (Cirac, 1987; Chalouan et al., 2014; Fassi 1999; Flecker et al., 2015) (Figure 1).

The Saïs basin contains foreland deposits dated from the middle Miocene to the Messinian. The late Miocene sediment series have been deposited in discordance either on the frontward side of the orogenic prism or on the African margin (Capella et al., 2018b).

During the mid-Tortonian, the paleogeography of the Rifian corridor was strongly controlled by thin-skinned tectonic processes, as a result of the simultaneous development of the Betic-Rifian progression systems (Morley, 1993; Platt et al., 2003) driven by the accentuated westward convergence of the Alboran microplate (Vergés and Fernàndez, 2012; Van Hinsbergen et al., 2014; Capella et al., 2018b).

During the late Tortonian, between 8.37 and 7.92 Ma, the prerif nappes were installed in the current zones in the Saïs and Gharb basins, inducing the flexure of the marginal foreland and generating open marine conditions that could be synchronous in the Rifian Corridor and which would occur at about 8.00–7.80 Ma (Krijgsman et al., 1999; Hilgen et al., 2000a, 2000b; Dayja et al., 2005; Capella et al., 2017a).

Since 8 Ma, the sedimentation in the Saïs basin was characterized by a widespread deposition of "blue marls" with various terrigenous intercalations (Wernli, 1988; Krijgsman et al., 1999; Gelati et al., 2000; Hilgen et al., 2000a, 2000b; Dayja, 2002, 2005;Bachiri Taoufiq et al., 2008; Achalhi et al., 2016; Capella et al., 2017b). This succession also contains carbonate facies that occur on the southeast margin of the Saïs Basin and Gulf of Skoura (Charrière and Saint-Martin, 1989; Saint-Martin and Charrière, 1989). bathymetrical estimations from benthic foraminifera of marly sequences in Saïs basin suggest that the maximum depth was 400–600 m at the end of the Tortonian (Dayja, 2002).

Mesozoic steep-fauls activity in the Rifian corridor basins, such as the Sidi Fili and Ain Lorma faults between the Gharb and Saïs basins (Figure 1), participated in the formation of ridge fold (Sani et al., 2007). The position of these faults is the main factor controlling the paleoflow and sediment repartition in the Late Tortonian (Capella et al., 2018b). During the late Tortonian and early Messinian, an intense tectonic induced the reactivation of steep faults in the African lithosphere (Morley, 1987; Gomez et al., 2000; Sani et al., 2000, 2007; Capella et al., 2017a). This event triggering localized uplift that again reduced the Rifian Corridor to depocenters bounded by shallow sills. This change in tectonic system is mainly related to a relative increase in convergence between Africa and Europe (Morel, 1989; Frizon de Lamotte et al., 1991; Jolivet et al., 2006).

At the early Messinian, the North Rifian corridor was emerged area, water exchange between the Atlantic and the Mediterranean was done through the South Rifian corridor. Marine sediments are encountered only in the deepest deposits of this corridor, such as Guercif, Saïs and Gharb.

A reconstitution of the paleoenvironment has been proposed by Capella et al. (2018a,b) for the Aïn Loma region. They indicate that this area is characterized by a paleoenvironment from the outer shelf to upper slope depth at the early Messinian.

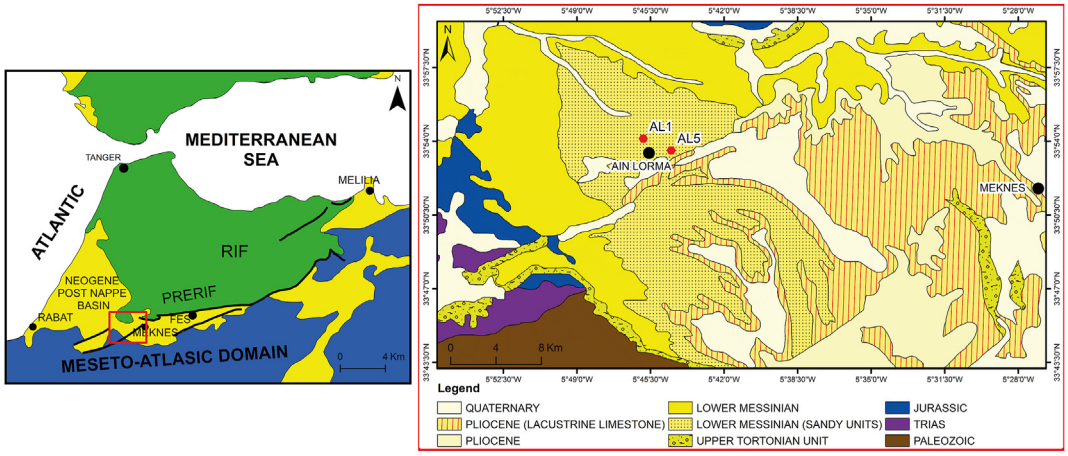

Figure 1. Location and geological setting of Saïs basin, South Rifian corridor, Morocco (Extract from geological map of the Rif (1/500000; after Suter, 1980).

3. Material and methods

3.1. Material

The boreholes studied are located in the Aïn Lorma region, at the West of the Saïs basin (Figure 1). The samples were collected from two boreholes, Al-1 and Al-5, drilled by the National Office of Hydrocarbons and Mines (ONHYM) In the context of exploration Mesozoic and Paleozoic substratum. Overall, the sampling resolution is between 1m and 20m. We studied all the available samples that ONHYM confided to us.

The borehole AL-1**(33°53′57.89″N, 5°45′44.58″O)** is located along the Rabat-Meknes Road, 1 km west of Ain Lorma. This is the first exploration drilling in the Ain Lorma area. The second borehole, Al-5**(33°53′24.31″N, 5°44′24.71″O)** is situated about 1400 m from Al-1, in the south-east of the Ain Lorma region.

3.2. Micropaleontology

The samples were washed and sieved according to the method in use.

The washing is carried out under running water on a column of four sieves, in the meshes are respectively 250μm, 160μm, 100μm and 63μm. The residue from each sieve is collected in a beaker and then dried in the oven at a temperature below 40 °C. Qualitative and quantitative analysis is executed on a fraction containing at least 300 individuals of planktonic foraminifera in the 160 μm fraction. In order to obtain information on paleoenvironments, two ecological indices were calculated: Pelagism index or planktonic-benthic ratio (P/P + B) and Diversity index.

***P/P + B ratio**

This ratio expressed as a calculation of P/(P + B) x 100 (the percentage of planktonic foraminifera of total foraminiferal population) is commonly used for paleobathymetric reconstructions (Gibson, 1989) and also provides information on the upwelling phenomena that promotes high productivity (Mathieu, 1986, 1988). In fact, information deduced from the works of Van der Zwaan et al. (1990), Van Hinsbergen and al., 2005, and Drinia and et al., 2004, 2007, shows that the P/B ratio is not always a reliable indicator of paleobathymetry.

It is recommended to consider the paleoecology of benthic foraminifera in the estimation of paleobathymetry according to the regression formula of Van Der Zwaan and al. (1990).

***Diversity**

Species diversity in planktonic foraminifera assemblages is based on the Shannon-Weaver function (Shannon and Weaver, 1949). The Shannon diversity index is commonly used to characterize species diversity in a population.

$$I_{SC} = -\sum(qi / Q \times Ln\ qi / Q)$$

$\mathbf{I_{sc}}$ = Shannon's diversity index
qi = Number of individuals counted for each species
Q = total number of species in the community

Shannon's index accounts for both abundance and uniformity of the species present (Daget., 1979; Murray, 1991).

3.3. Palynology

Al-1 borehols samples were prepared using the standard palynological method with the following process:

- Multiple HCL (20%) and HF (40%) attacks to eliminate carbonates, silicates and fluorosilicates. Samples must be neutralized after each acid treatment using distilled water.
- Sieving at 10 μm in order to remove any remaining silt and clay particles.
- The resulting residues have been mounted between slides and lamellae.

The palynological analysis of Al-5 borehole has not been carried out in this work. However, samples are currently under processing.

At least 160 pollens excluding Pinaceae have been counted. Percentages of each taxa were calculated with regard to the sum of all pollen grains.

Frequencies of each taxon are shown in a detailed pollen diagram. The pollen taxa have been grouped into a synthetic diagram according to the ecology of their representative (Suc, 1984, 1989).

In the case of the dinoflagellates, 90 cysts have been counted at least. The relative proportions of each dinokyst taxa appear in a detailed diagram.

3.4. Bioclimatic markers of continental environments

The average annual temperature (Tann) can be estimated from current ecological conditions using the following plant groupings (Nix 1982): megatherm elements (24 °C), mega-mesotherm elements (20–24 °C), mesotherm elements (14–24 °C) and microtherm elements (10–14 °C). For humidity, either the Poaceae/Compositae ratio (Cour and Duzer 1978) may be used, or apply a transfer coefficient to pollen data relative

both to their frequency and the current climatic parameters of taxa (Fauquette et al., 1998).

3.4.1. Megatherms (tropical)

The megatherm group includes *Avicennia*, Sapindaceae, Icacinaceae, Acanthaceae and Euphorbiaceae.

3.4.2. Megamesotherms (subtropical)

This group includes Taxodiaceae, *Engelhardia*, Sapotaceae, Arecaceae and *Cathaya*, **Mesotherms (hot-temperate)**.

This groups made up of *Alnus, Deciduous Quercus*, *Carya*, *Ulmus*, *Populus*, *Buxus* type sempervirens, *Carpinus*, *Ulmus*, *Rhus*, *Juglans*.

3.4.3. The Poaceae/Compositae ratio

The annual precipitation variation may be estimated via a ratio between two regularly occurring taxa that have opposite climatic significance (Cour and Duzer, 1978). In xeric environments, it is necessary to use the ratio between Poaceae and Compositae (Cour and Duzer, 1978). Poaceae clearly predominate (ratio >20) when annual precipitation exceeds 500 mm; in contrast, Compositae predominate (ratio <20) when annual precipitation is less than 500 mm. The proportion between those two principal components of herbs provides a faithful reflection on humidity variation. Dry conditions promote the growth of Compositae while wet conditions favor Poaceae development; except for one Poaceae, the *Lygeum* genus, which currently lies under arid climate conditions characterized by an annual average temperature between 16 and 21 °C and an annual average rainfall of about 150–400 mm (Fauquette et al., 1998).

3.5. Index of marine environment

3.5.1. Distality index

For the purpose of understanding how sea level variations may affect the Saïs Basin during the TMT, the following indicator has been applied:

- The synthetic diagram with *Pinus* + undeterminable Pinaceae in which these taxa (favored by transport) are opposed to halophytes (coastal plants). The abundance of Pinaceae is increasing in distal areas and decreasing in proximal ones (Heusser and Balsam, 1977; Suc and Drivaliari, 1991). In contrast to Pinaceae, the Halophytes provide useful indicators of coastal environments.
  - D/S ratio (D: Dinokysts and S: Spores + Pollen) is used to evaluate the marine influence relative to the continental influence (Warny, 1999).
- The G/P curve obtained from Gonyaulacoid and Peridinoid ratio can be used to detect the in-shore-of-shore direction (Warny, 1999) (G:Gonyaulacoïdes (*Spiniferites* spp), Peridinoid (*Selenopemphix nephroides*)).
- The distality index IN/ON represents the ratio of inner platform néritic assemblies to outer platform neritic assemblies. ON is expressed as the sum of all values of *Spiniferites* spp. IN stands for *Operculodinium israelianum*, *Lingulodinium machaerophorum*, *Polyspheridium zoharyi*, *Tuberculodinium vancompoae*, *Tectatodinium pellitum.*

3.5.2. Temperature index

The index of sea surface temperature is evaluated by the ratio between warm water indicator dinocysts (W) (*Spiniferitesspp, Operculodinium israelianum, Lingulodinium machaerophorum, Polyspheridium zoharyi*, *Tuberculodinium vancompoae, Tectatodinium pellitum., Impagidinium patulum, Impagidinium acuuleatum*, Peridiniaceae) and cold water dinocysts taxa (C) (*Operculodinium centrocarpum, Impagidinium sphearicum, Nematosphaeropsi slemniscata, Nematosphaeropsis Labyrinthea, Bitectatodinium tepikiense*).

3.6. Palynofacies

Two groups of organic matter are identified, structured and unstructured elements (Poumot and Suc, 1994).

- **Structured elements**

This group is composed of well identifiable vegetal organisms and can be divided into woody organic matter (WOM) and cellular organic matter (COM).

- **Unstructured elements**

The original organic matter has submitted to a physic-chemical transformation, we distinguish black organic matter (BOM) and amorphous organic matter (AOM).

4. Results

4.1. Lithological description of the boreholes studied

4.1.1. Al-1 borehole

The Al-1 borehole starts directly in the grey marls, from the bottom to the top of the hole, we observe (Figure 2):

From 592 m to 471 m: finely brown marls sandstone with lignite traces
From 471 m to 425 m: red marls sandstone
From 425 m to 405 m: fine grey sandstone
From 405 m to 350 m: grey marls sandstone
From 350 m to 25 m: grey marls
From 25 m to 1 m: yellow clay

These sedimentary deposits were attributed to the Middle Miocene according to unpublished ONHYM reports.

This sedimentary series was intensively sampled, according to the available samples, between the depths 545 m and 6 m.

4.1.2. Al-5 borehole

The Al-5 borehole starts in the Saïs fluvio-lacustrine complex; from the bottom to the top, we distinguish (Figure 3):

From 658 m to 435 m: red marls to anhydrite with sandstone inter layers
From 435 m to 65 m: sandy gray marls
From 65 m to 30 m: sandy yellow clays with yellow sandstone layers
From 30 m to 0m: fluvio-lacustrine complex

The age was probably proposed from the seismic data (according to the preliminary drilling report). The authors attributed these sediments to the Middle Miocene (Langhian - Serravallian).

The samples obtained are located between 75m and 514m. Unfortunately, we could not get the samples between 0 and 75m.

The dating proposed for these boreholes is old, hence the interest in updating the biostratigraphic framework of these sedimentary deposits.

4.2. Biostratigraphic results

Biostratigraphical analysis is based on the qualitative and quantitative study of planktonic foraminifera associations. Specific identification is carried out on the basis of specialized references (Wernli, 1988, Iaccarino, 1985, Barhoun and Wernli, 1999, 2000, Iaccarino et al., 2007; Sierro et al., 1987, 1993, 1997).

The washed residues reveal rich and diverse microfauna. The residues are composed of planktonic and benthic foraminifera, some ostracods, fragments of bivalve shells and echinoderms radioles. The planktonic microfauna is well preserved, presenting a frosty appearance (Antonarakou et al., 2019) and well suited for biostratigraphical study.

In order to highlight the biostratigraphic events, we performed a complete count in a portion containing approximately 300–400 individuals from the fraction 160 μm of each sample. The taxonomic

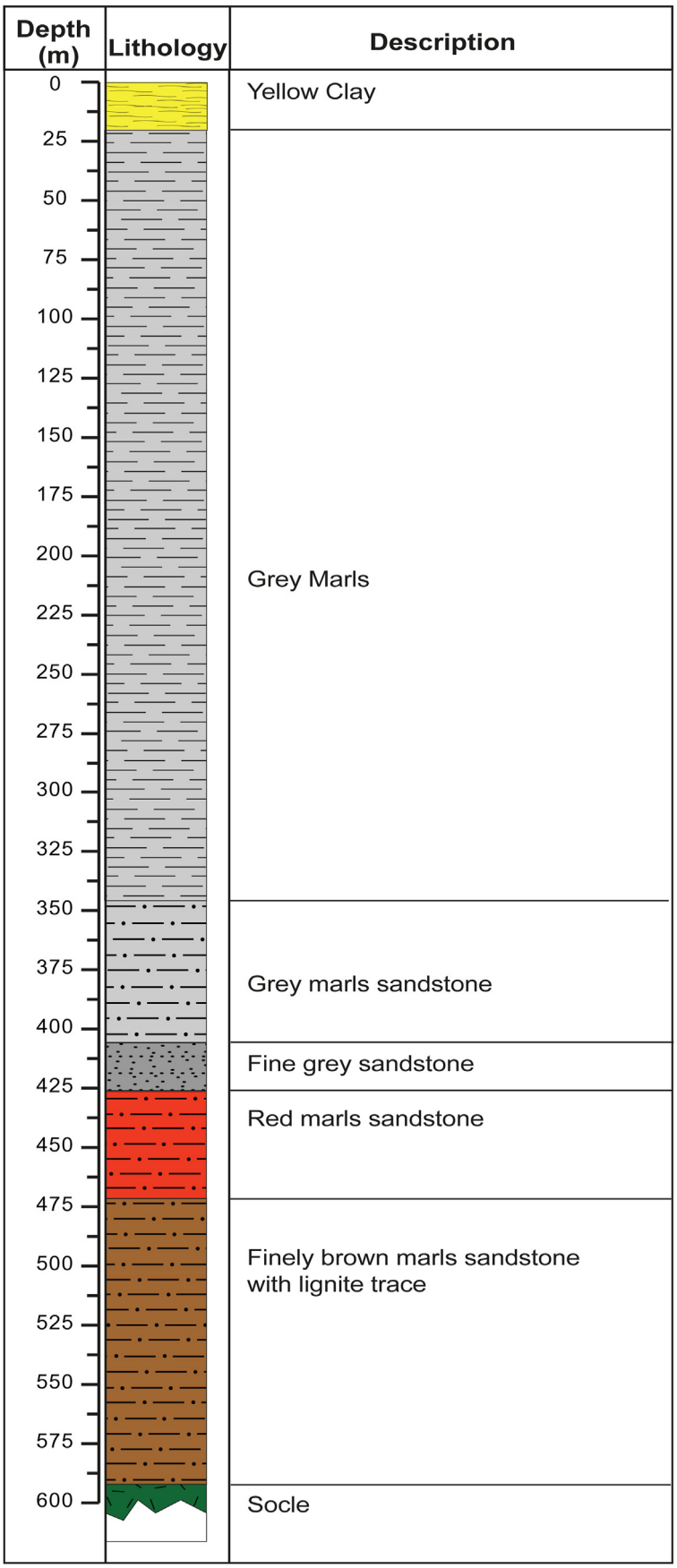

Figure 2. Lithological description of Al-1 borehole.

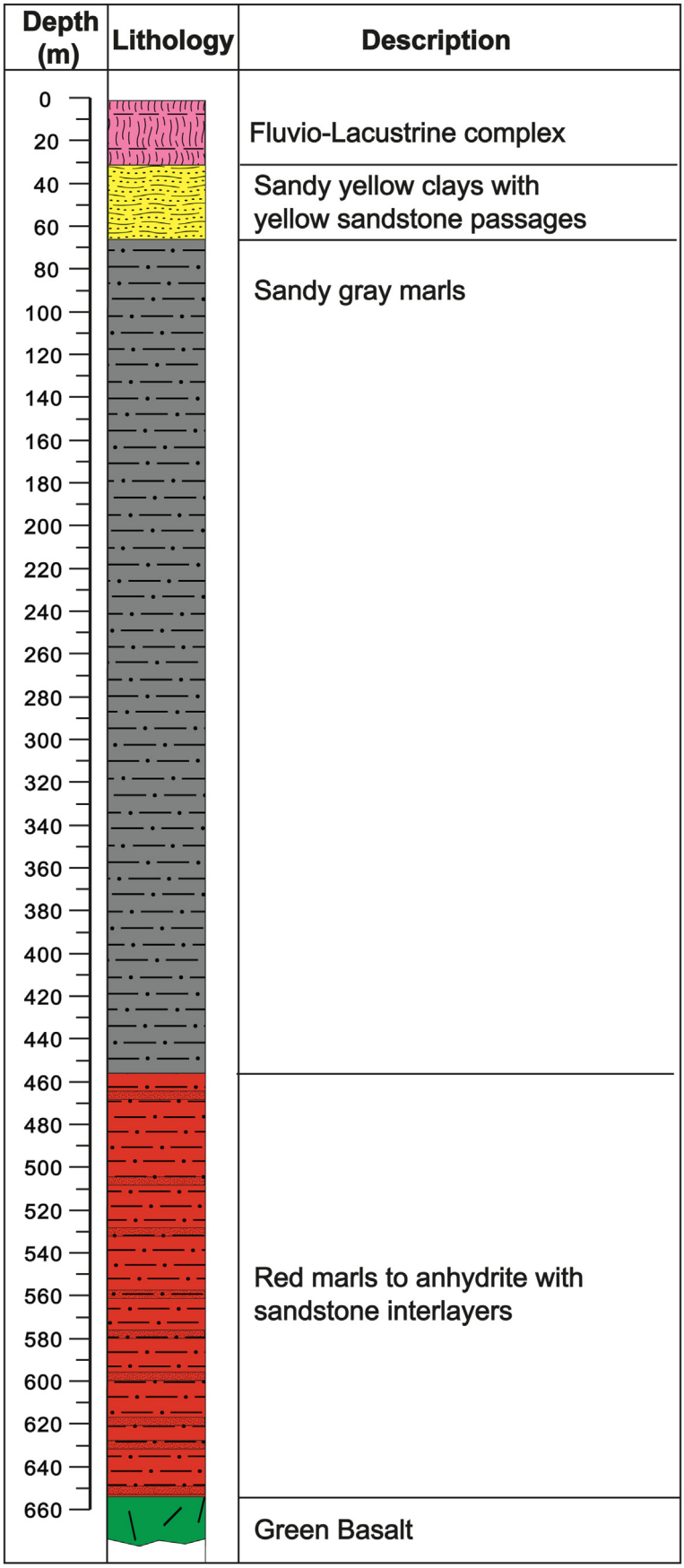

Figure 3. Lithological description of Al-5 borehole.

approach adopted in this work has considered, in addition to the vertical distribution of the marker species, coiling changes of *Globorotalia menardii*, *Globorotalia scitula* gr., *Globorotalia miotumida* gr. and *Neogloboquadrina*, and the presence or absence of keeled and non-keeled *Globorotalia*.

In order to improve the chronostratigraphical framework of the studied sedimentary successions, we have adopted high-resolution biostratigraphy calibrated to the astronomical time-scale recently used in the Mediterranean and adjacent Atlantic domain (Sierro, 1985; Sierro et al., 1993, 2001; Hilgen et al., 1995, 2000a, 2000b; Krijgsman et al., 1995; Lourens et al., 2004). The astronomical correlation of Ain El Beida and oued Akrech sections (Atlantic coast, Morocco) reveals that the bioevents have a similar age as those distinguished in the Mediterranean area (Hilgen et al., 2000a; Krijgsman and Garces, 2004).

4.2.1. AL-1 borehole planktonic foraminiferal assemblages description and biostratigraphy

The micropaleontological study of the sediments from AL-1 borehole revealed a remarkable richness in species and individuals. In all, 26 species belonging to 12 genera were identified.

The planktonic foraminifera assemblages are characterized by high diversity at depths ranging from 545 m to 195 m with a Shannon diversity index varying from 2 to 2,5, especially between 439 and 195 m (Figure 10). This diversity becomes relatively moderate between 195m and 6m (the Shannon diversity index oscillates from 1,5 to 2). The planktonic-benthic ratio varies between 60% and 85% in the lower part of the borehole (from 400m to 195m) and decreases significantly at the top of the borehole, from 186m to 6m with percentages comprised between 70% and 42%.

The vertical distribution of planktonic foraminiferal species is illustrated in Figure 4.

4.2.2. AL-5 borehole planktonic foraminiferal assemblages description and biostratigraphy

Detailed analysis of Al-5 borehole reveals well-diversified planktonic foraminiferal associations.

In total, twenty-three species belonging to 10 genera have been identified. The residues are consisting of planktonic and benthic foraminifera, some ostracodes, bivalves fragments and echinoderms radioles.

The planktonic assemblages are characterized by moderate to higher diversity, with a Shannon diversity index varying between 2.4 and 1.7 (Figure 5). The plankton-benthic ratio stands between 60 and 80% in the bottom of the borehole (from 514 to 315m depth), while it reaches 0–60 % between depths 315 and 75m.

The vertical distribution of the planktonic foraminiferal species is presented in Figure 6.

4.2.3. Biostratigraphical events in Al-1 and Al-5

From the qualitative and quantitative analysis of the planktonic foraminifera associations in all studied samples and the stratigraphical distribution of markers species (*Globorotalia menardii*, *Globorotalia miotumida*, *Globorotalia conomiozea*, *Globorotalia scitula* and *Neogloboquadrina acostaensis*), we have identified five bioevents (Table 1). Four of them are common between the two boreholes. The distinction of such biostratigraphical events within the studied boreholes allowed us to pinpoint the late Tortonian, the Tortonian-Messinian boundary and the early Messinian. The events recorded in the two recorded boreholes are:

1 Last common occurrence (LCO) *Globorotalia menardii* 4 (7,51 Ma);
2 First common occurrence (FCO) *Globorotalia menardii* 5 (7,35 Ma);
3 S/D coiling change of *Globorotalia scitula;* (7,28 Ma);
4 Replacement of *Globorotalia menardii* 5 by *Globorotalia miotumida* group (7,25 Ma)

We have noted that the quantitative evolution of the *Globorotalia miotumida* group reveals the influx of *Globorotalia miotumida (conomiozea)* around 161m in borehole Al-1. This auxiliary event has been reported by Lourens et al. (2004) and Sierro et al. (2001) with age 7.20 to 7.18 Ma.

Furthermore, the evolution of *Neogloboquadrina acostaensis* throughout the two boreholes indicates that its coiling is preferentially sinistral.

We looked very carefully for *Globorotalia nicolae* within *G. scitula* gr, but we did not observe it. We also found that the *Globorotalia miotumida* group is present up to the top of both boreholes (6m in borehole Al 1 and 75m in borehole Al-5).

Therefore, Messinian sediments are probably deposited before the LO *Globorotalia miotumida* gr. (6.52 Ma), or possibly before FO *G. nicolae* (6.83 Ma).

The lacuna of samples between 0 and 6m in borehole Al-1 and between 0 and 75m in borehole Al-5 could explain the absence of the following events: FO *Globorotalia nicolae* (6.83 Ma), LO *Globorotalia nicolae* (6.72 Ma), LO *Globorotalia miotumida* gr. 6.52, FCO *Turborotalita multiloba* 6.42 Ma and S/D *Neogloboquadrina acostaensis* (6.35 Ma).

From these biostratigraphic bioevents, we may date the Al-1 borehole from the Upper Tortonian-Messinian and locate the Tortonian-Messinian boundary at about 195 m (The estimated age is between 7.8 Ma and 6.52 Ma).

The Al-5 borehole can be attributed also to the late Tortonian - early Messinian, with an estimated age ranging between 7.8 Ma and 6.52 Ma.

4.3. Palynological results

The detailed palynological analysis of Al-1 borehole reveals a significant richness in both pollen and dinoflagellate cysts.

4.3.1. Terrestrial inputs

This area has a diverse and relatively abundant pollen flora. Almost 12536 palynomorphs were counted in 28 samples and a total of 72 pollen taxa were identified. The detailed and synthetic diagrams (Figures 8, 10) reflect a very homogeneous floristic picture during the Upper Miocene.

The megatherm group is represented by *Avicennia*, Sapindaceae, Icacinaceae and Euphorbiaceae. These elements are present in a sporadic to rare occurrence *(0 to 4.7%)*.

As for the mega-mesotherms, Taxodiaceae and *Engelhardia* pollen grains are predominant; the other elements of this group are present infrequently and sporadically (e.g. *Hamamelidaceae* 0–3 %).

Mediterranean flora elements are preponderant as, their percentages reach 50%. They are mainly represented by *Olea* (22.7%), *Quercus Ilex-coccifera* type (9%) and *Ziziphus* (3.19%).

Mesotherms as a whole are dominated by Deciduous *Quercus* (9%), nevertheless the other species such as *Ulmus*, *Populus*, *Buxus sempervirense*-type, etc. are discontinuously represented with low percentages.

Cathaya pollen grains are present all along the borehole with percentages reaching 15%, while Cupressaceae occur discontinuously.

The highest percentages were observed for herbaceous plants and Pinaceae, although those have declined at 275 m, 256 m–235 m, 205 m–186 m (boundary Tortonian Messinian), and 100 m.

The herbaceous plants are very abundant, they represent more than 80%. Among this group of taxa we can find Compositae (43%), Brassicaceae (21%), and Poaceae (20.4%).

Environmental dryness is indicated by the occurrence of sub-desert elements such as *Lygeum*, *Calligonum*, *Erodium*, *Ephedra* and *Artemisia*, where *Lygeum* (1.44%) and *Ephedra* (3%) are predominant.

Halophytes are represented by Amaranthaceae (0 à 10.17 %), Caryophyllaceae (<1%) and Plumbaginaceae (up to 2%). It should be noted that Amaranthaceae pollens become very frequent at levels 205 m and 186 m (boundary Tortonian Messinian) where they reach the value of 7.06–10.17 %.

The abundance of Pteridophytes spores (11–50%) and the presence of *Concentricystes* attest the influence of fluvial inputs.

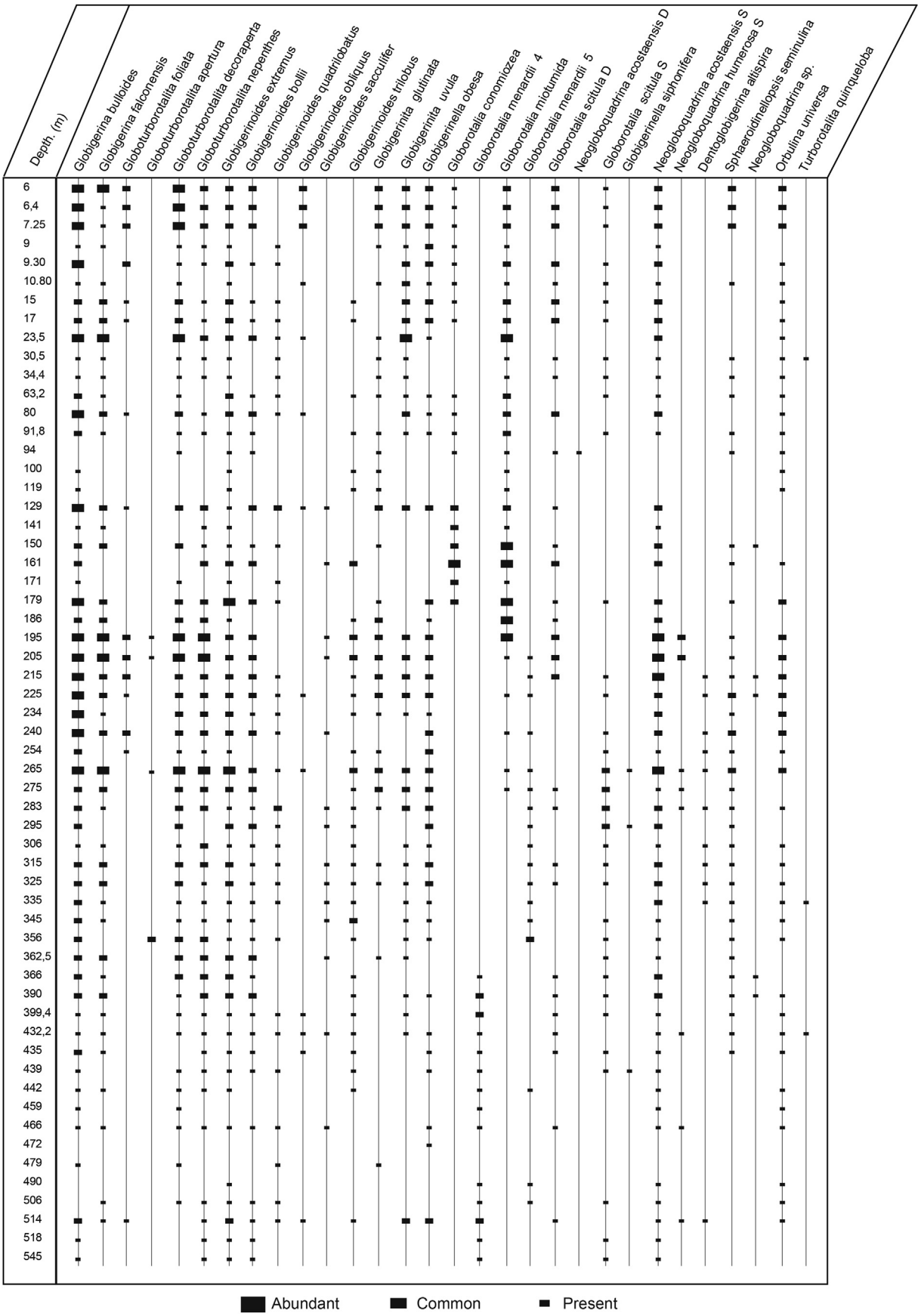

Figure 4. Distribution of planktonic foraminifera of Al-1 borehole.

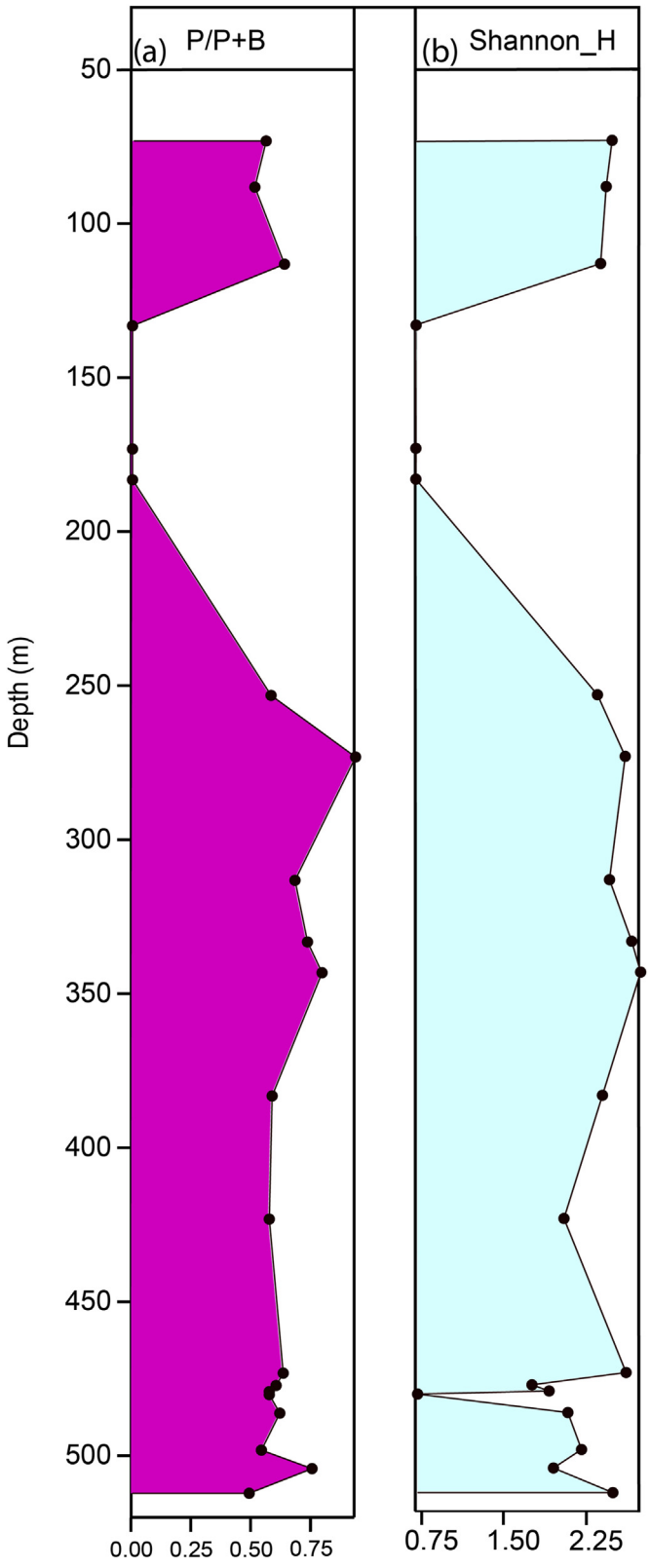

Figure 5. Ecological parameters of Al-5 borehole: (a) P/P + B ratio; (b) Diversity Index.

Reworked pollens are distributed alongside the borehole, their percentages increase in the lower Messinian at 100 m level where they reach 4%.

4.3.2. Marine inputs

Dinoflagellate cysts excavated from Ain Lorma borehole (Al-1) were very plentiful and very widely diversified. For each slide, an average of 90 dinoflagellate cysts was identified and counted per each slide (Figure 9).

At the late Tortonian (518 m–195 m) D/S curve (Dinocyst/(pollen + spore)) has low to medium proportions varying from 0.16 to 0.57 (Figure 10). Thus, terrestrial palynomorphs present high concentration compared to the concentration of the dinocysts taxa. The G/P curve reveals an average value of 0.9 across the whole plot (Figure 10). In fact, Gonyaulacoid are predominant while Peridinoid are poorly represented.

The dinocyst assemblages mainly consist of 10–40 % by *Spiniferites spp*. (including the following species *S. mirabilis*, *S. membranaceus*, *S. ramosus*, *S. granulatus*, S. *pseudofurcatus*, S. *hypercanthus*, *S. pachyderma*), Achomosphera spp. (5–20%), *Operculodinium israelianum* (1–16 %), *Lingulodinium machaerophorum* (0–15,69 %), *Polysphaeridum zoharyi* (3–15%), *Operculodinium centrocarpum* (0–6%), *Operculodinium Jeaduchenei* (0–8%) (Figure 9). Oceanic taxa (*Impagidinium*) are weakly represented (0–8%). Acritarches are frequently found (0–17%). Foraminiferal chitinous tests are rarely encountered; their percentage varies between 0 and 1.5% (Figure 9).

At the T/M boundary, it is noticed that D/S value is low and declines from 205 m, arriving to 0.16 then ascends to 0.33 at 195m before falling again to 0.14 at 186m. Similarly, the percentage of Pinaceae decreases at 205 m, then it slightly increases at the T/M boundary lying at 195 m, before decreasing further at 186 m (Figures 8, 10). Halophytes evolves inversely to Pinaceae, their frequencies increase at the 205 m and 186 m levels and decrease at the 205 m level.

In comparison to the Tortonian, we observe at the T/M, a significant change in the dinoflagellate cyst associations. *Spiniferites* frequency decreases such that it attains 13,84%, those of *Achomosphaera spp.* and *Operculodinium israelianum* à 3%. Nevertheless, the percentage of *Impagidinium* rises to 10%, *Nematosphaeropsis lemniscata* and *Nematosphaeropsis labyrinthus* reach 6%, *Operculodinium janduchenei* achieves 14% and *Operculodinium oriensum* 10.77% (Figure 9).

In the early Messinian, the D/S curve (terrestrial input abundances) appears low between 186 and 26.5 m, varying between 0.14 and 0.44. The Dinokyst association is composed of the identical taxa found in the Tortonian (Figure 9). Compared to the T/M limit, the early Messinian is distinguished mainly by an upward trend in *Spiniferites*, *Achomosphaera spp.* and *Operculodinium israelianum*. Furthermore, there is also a reduction in the frequency of *Impagidinium*, *Nematosphaeropsis spp.*, *Operculodinium janduchenei* and *Operculodinium oriensum*. These taxa increase once more at the 100 m layer. W/C curves fluctuate between 0.89 and 0.98 (Figure 10).

4.3.3. Palynofacies evolution

Throughout this marly series, no major variations in palynofacies were observed (Figure 10). There is an almost uniform prevalence of black organic matter ("BOM "), cellular organic matter (" COM" which predominates at 195 m, T/M) and woody organic matter "WOM". BOM is the most important element (especially in early Messinian), its proportion varies between 11 and 50%. For the COM and WOM the same values are also found. Amorphous organic matter (AOM) represents the lowest percentage, except at 376 and 283 m it can arrive 40%.

5. Discussion

After presenting a biostratigraphic synthesis of the boreholes studied, the results obtained in this work and their integration into the data known elsewhere will be discussed in two successive aspects. Firstly, we expose the temporal evolution of marine environments with reference essentially to foraminifera and dinokysts. While the second aspect treats the continental environments (vegetation) from the pollen record.

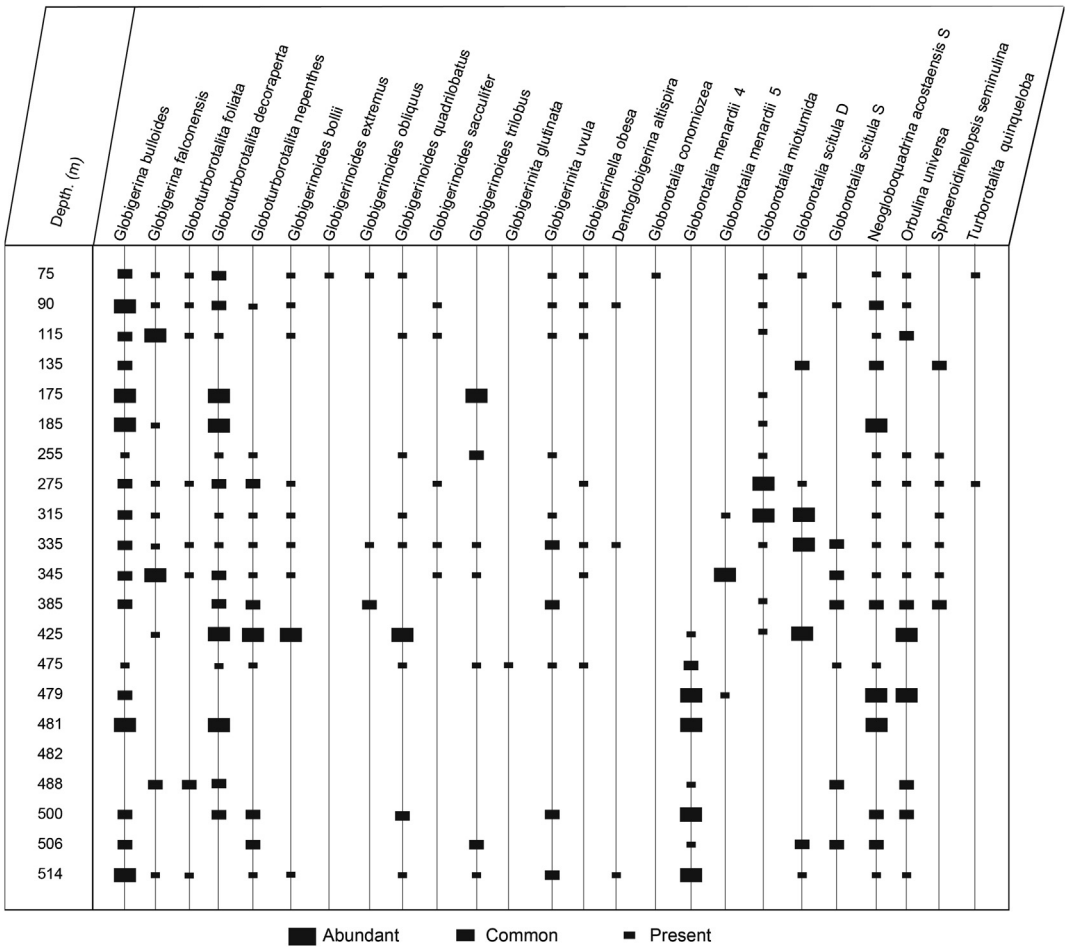

Figure 6. Distribution of planktonic foraminifera of Al-5 borehole.

Table 1. Main planktonic foraminiferal bioevents used to date AL-1 and AL-5 boreholes. References are for the astronomically calibrated ages in the Mediterranean region and its Atlantic side.

Age	Biovents	Al-1 borehole	Al-5 borehole	Chronostratigraphy Age (Ma)	References
Early Messinian	High conical *Globorotalia miotumida* group	161 m	Absent	7, 18-7,20 Ma.	Sierro et al. (2001); Lourens et al. (2004)
Late Tortonian	Replacement of *Globorotalia menardii* 5 by *Globorotalia miotumida* group	195 m	315 m	7.25 Ma.	Sierro (1985); Sierro et al. (1993), 2001; Tulbure et al., (2017)
	Sinistral to Dextral coiling change of *Globorotalia scitula*	215 m	335 m	7.28 Ma	Sierro (1985); Sierro et al. (1993); Hilgen et al. (2000a), 2000b, Tulbure et al. (2017)
	First common occurrence (FCO) of *G. menardii 5*	356 m	345 m	7.35 Ma	Sierro (1985); Sierro et al. (1993); Hilgen et al. (1995); Hilgen et al. (2000a), 2000b; Krijgsman et al. (1995); Lourens et al. (2004), Tulbure et al. (2017), Lirer et al., (2019)
	Last common occurrence (LCO) *Globorotalia menardii 4*	366 m	425 m	7.51 Ma.	Sierro (1985); Sierro et al. (1993); Hilgen et al. (1995); Hilgen et al. (2000a), 2000b; Krijgsman et al. (1995); Lourens et al. (2004), Tulbure et al. (2017), Lirer et al., (2019)

5.1. Biostratigraphic synthesis

In the present work, we applied high-resolution biostratigraphy calibrated to the astronomical scale recently used in the Mediterranean area. This method allows precise dating and correlation between several areas (Hilgen et al., 1995; Krijgsman et al., 1994; 1999; Sierro et al., 2001; Lourens et al., 2004; Hilgen et al., 2012 in Gradstein et al., 2012; Lirer et al., 2019). This biochronology is very similar to that developed for the adjacent Atlantic domain by Sierro (1985) and Sierro et al. (1993). The biostratigraphic events identified in this study are commonly used in the Mediterranean and adjacent-Atlantic domains. They are also in agreement with previous work realized in Morocco.

5.1.1. Late Tortonian

This interval is characterized by the succession of three bioevents: LCO *Globorotalia menardii* 4 (sinistral form), FCO *Globorotalia menardii* 5 (dextral form) and coiling change from sinistral to dextal form in *Globorotalia scitula* group.

The evolution of the percentage of *Globorotalia menardii* form 4 reveals that this species is present from the base in both drill holes,

becomes sometimes abundant to its reduction then its disappearance at the level of 366m in drill hole Al-1 and 425m in drill hole Al-5 (Figures 4 and 6). The bioevent, LCO *Globorotalia menardii* 4 with an age of 7.51 Ma, has been observed in the adjacent Atlantic by Sierro (1985), Sierro et al. (1993), Hilgen et al. (2000a, 2000b) and Lourens et al. (2004) and in the Mediterranean basin by Krijgsman et al. (1995), Krijgsman et al. (1999), Hilgen et al. (1995), Lirer et al. (2019).

The first common occurrence of *G. menardii* 5 was reported from 356m in borehole Al-1 and 345m in borehole Al-5. This event has been registered at 7.35 Ma in the Atlantic and Mediterranean domain (Sierro, 1985; Sierro et al., 1993; Krijgsman et al., 1995, 1999; Hilgen et al., 1995, 2000a, 2000b; Lourens et al., 2004; Lirer et al., 2019).

In our samples, the last presence of *G. menardii* 5 was observed around the Tortonian - Messinian boundary. In fact, the LCO *G. menardii* 5 (within astronomical age 7.23Ma) is recorded after the Tortonian-Messinian boundary (Lourens et al. (2004); Hilgen et al. (2000a, 2000b); Lirer et al., 2019). Kontakiotis et al. (2019) mentioned the disappearance of *G. menardii* 5 before the Tortonian-Messinian boundary.

Regarding non-keeled *Globorotalia*, we controlled the evolution of the percentage of sinistral and dextral forms in the *Globorotalia scitula* group in all the studied samples. Thus, the evolution of the dextral and sinistral forms of *Globorotalia scitula* gr. highlighted that the sinistral forms are more represented in the lower part of the two boreholes, and a change of coiling from sinistral to dextral of the *Globorotalia scitula* group was detected at depths of 215 m and 335 m respectively at boreholes Al-1 and Al-5. This bioevent has been previously reported by Sierro (1985), Sierro et al. (1993) and Hilgen et al. (2000a, 2000b). Its age is estimated at 7.28 Ma. However, in the Mediterranean area, this astronomical age is attributed to the Paracme end (PE) of *Globorotalia scitula* dextral bioevent (Lourens et al., 2004; Lirer et al., 2019; Kontakiotis et al., 2019).

5.1.2. Tortonian - Messinian boundary

The Tortonian/Messinian boundary is defined by the FCO *G. miotumida* gr (Hilgen et al., 2000a, b; Lourens et al., 2004; Lirer et al., 2019). at 7.24 Ma. On the other hand, the replacement of *Globorotalia menardii* form 5 by the *Globorotalia miotumida* group has been applied as a criterion to recognize the Tortonian-Messinian boundary (Sierro, 1985; Sierro et al., 1993, 2001). In the studied samples, the FRO of *Globorotalia miotumida* gr. Coincides with the disappearance of *Globorotalia menardii* 5, so we chose the bioevent that corresponds to the replacement of the *Globorotalia menardii* 5 by the *Globorotalia miotumida* group to identify the Tortonian-Messinian boundary. However, it is preferable to adopt the most commonly used event, FCO *Globorotalia miotumida* gr., to characterize the Tortonian - Messinian boundary.

5.1.3. Early Messinian

The base of the Messinian coincides with the FCO *Globorotalia miotumida* (7.24 Ma). We have noted that the quantitative evolution of the *Globorotalia miotumida* group reveals the influx of *Globorotalia miotumida (conomiozea)* around 161m in borehole Al-1. This auxiliary event has been reported by Lourens et al. (2004); and Sierro et al. (2001) with age 7.20 to 7.18 Ma.

We looked very carefully for *Globorotalia nicolae* within *Globorotalia scitula* gr. But we did not observe it.

We also found that the *Globorotalia miotumida* group is present up to the top of both boreholes (6m in borehole Al-1 and 75m in borehole Al-5). Therefore, Messinian sediments are probably deposited before the LO *Globorotalia miotumida* gr. (6.52 Ma), or possibly before FO *Globorotalia nicolae* (6.83 Ma).

The lacuna of samples between 0 and 6m in borehole Al-1 and between 0 and 75m in borehole Al-5 could explain the absence of the following events: FO *Globorotalia nicolae* (6.83 Ma), LO *Globorotalia nicolae* (6.72 Ma), LO *Globorotalia miotumida* gr. 6.52, FCO *Turborotalita multiloba* 6.42 Ma and S/D *Neogloboquadrina acostaensis* (6.35 Ma).

5.1.4. Studied boreholes correlation

The correlation of the boreholes studied showed variations in thickness and the appearance of emersion indices (Figure 7). In the late Tortonian, the thickness is 350m in borehole Al-1 and about 200m in Al-5. While for the early Messinian, the thickness variation is less pronounced, being around 189m in borehole Al-1 compared to 240m in borehole Al-5. Furthermore, the top part of Al-5 borehole was continental, as indicated by the presence of lacustrine limestone (from 0 to 30m). These continental conditions are absent from borehole Al-1, which remained marine until the top of the sedimentary series. This variation in thickness and the installation of lacustrine conditions could be explained by the activity of the faults well developed in the Ain Lorma region (Morel, 1988; Capella et al., 2018b).

5.2. Marine environments

Sea level variations throughout Saïs basin from the late Tortonian to the Lower Messinian will be proposed from the comparisons between the different markers found as illustrated in Figure 10.

5.2.1. Late Tortonian

The late Tortonian in AL-1 borehole extend from 518 m to 195 m, and is distinguished by three successive bioevents: LCO *G. menardii* 4 (sinister form) at 7.51 Ma, FCO *G. menardii* 5 at 7.35 Ma, and coiling change from sinister to dexter of *G. scitula* gr., S/D at 7.28 Ma.

From 7.51 to 7.28 Ma the microfauna of the marine sediments of the Al-1 borehole is rich and well diversified (ID high 2.5 to 3), its attests to a marine environment favorable to the development of the plankton population. The P/P + B ratio fluctuates between 70 and 80% that indicates an open marine environment relatively deep, and the G/P ratio varies between 0.9 and 1 and reflects the same conclusion (Figure 5, 10).

The dinokyst assemblages, the abundance of pollen grains, spores, cellular organic matter, black organic matter and the occurrence of *Concentricystes* reflect a marine environment very close to the continent, with significant fluvial inputs (D/S is low ranging from 0.16 to 0.57). Vegetation cover does not appear to be dense which may have facilitated soil drainage from streams into the depositional environment.

Oceanic taxa (*Impagidinium sp.*) are poorly represented. Distality markers (DI, pinaceae) reveal a distal neritic environment with proximal trends especially at 275 m, in which the distality index increases and reaches 0.73. The sea surface temperature is warm, as illustrated by the temperature index, which comes above 0.9 at most levels. However, the distality curves show trends toward an internal environment, probably related to tectonic instability in this region (where tectonic forcing is possibly superimposed on glacio-eustatic forcing) as the global sea level change curve during the Tortonian period indicates a high sea level (Haq et al., 1987). These results are in agreement with recent data from Capella et al. (2017a, 2018b, 2019a, 2019b) and Sani et al. (2007) which point out that between 8 Ma and 7.25 Ma, a remarkable change occurred, from the subsidence of the basin to the thick-skinned contraction causing an inversion of the normal faults (of the Mesozoic of the African margin) oriented NS towards NE-SW.

Previous results obtained from foraminifera (Barhoun, 2000; Dayja, 2002), ostracods (Kili, 1993) and palynology (Bachiri Taoufiq, 2000) confirm also an environment relatively deep (maximum depth was 400–600 m at the end of the Tortonian (Dayja, 2002)) with an open distal environment, with little fluctuations, to a proximal environment. At Bou Regreg (North-Western Morocco), the environment is naturally oceanic and the isotopic curve indicates a high sea level (Warny et al., 2003). The associations of dinokysts in BouRegreg are similar to those found in the Saïs Basin. During the late Tortonian, Boudinar and ArbaaTaourirt basins (Northeastern Morocco), corresponded to a shallow marine environment (Achalhi et al., 2016).

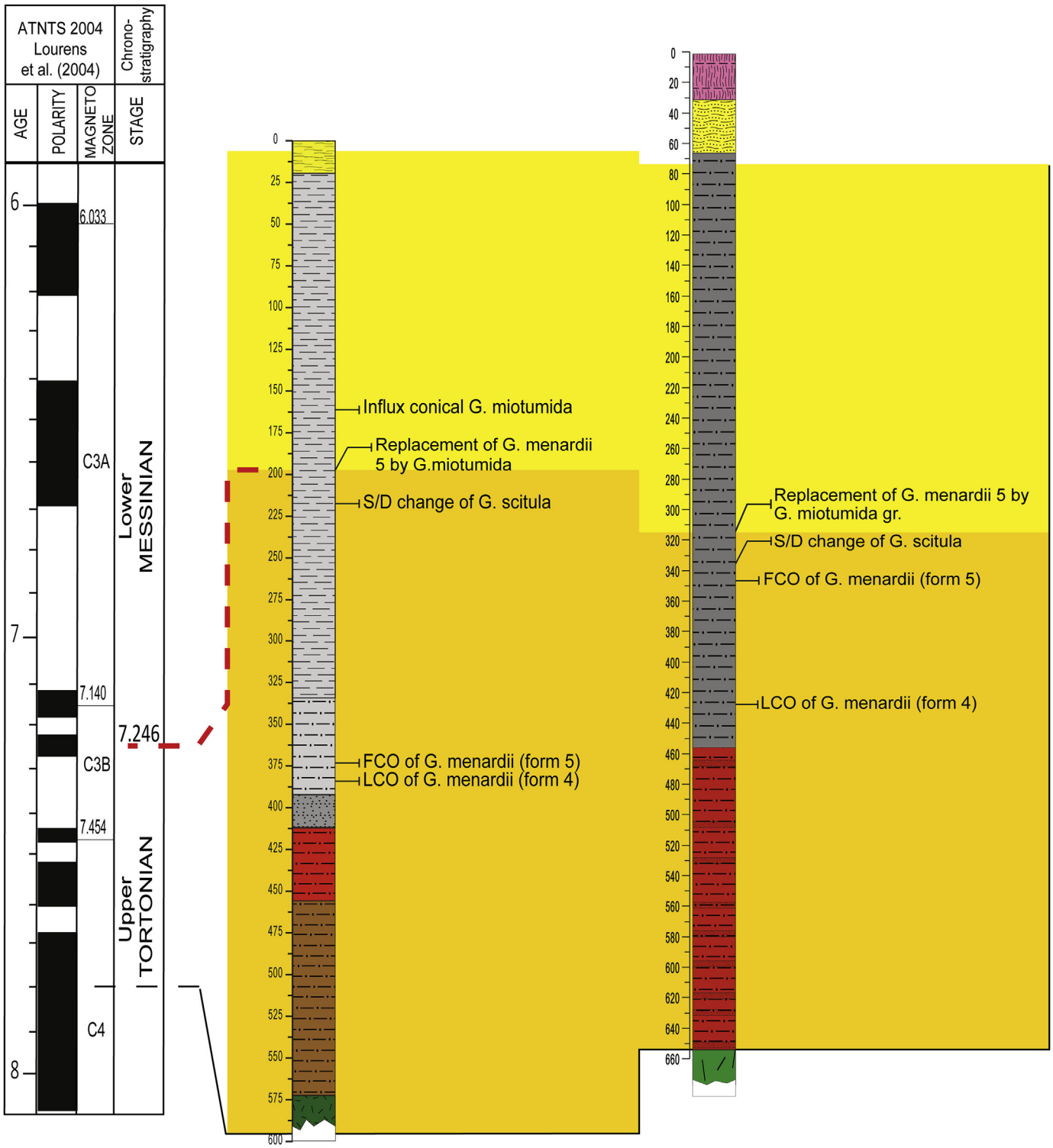

Figure 7. Biostratigraphical correlation of the studied boreholes.

5.2.2. *Tortonian/Messinian boundary*

The replacement of *G. menardii*5 (dextral) by *G. miotumida* was spotted at a depth of 195 m and helped to pinpoint the Tortonian-Messinian boundary. This limit is characterized by a lower diversity index than previously, so the foraminifera diversity has relatively decreased, although marine conditions remain favorable to proliferation of microfauna. The P/P + B ratio is about 70%, expressing an open and relatively deep marine environment.

The D/S ratio remains low at 0.33, representing an epicontinental environment dominated by high fluvial inputs.

The IN/ON (distality index) ratio comes to 0.6. Proximal neritic taxa are predominant. The environment inferred is neritic proximal with a tendency towards an inner platform environment. Pinaceae also show a decrease confirming this trend. This great change in the direction of impoverishment of the microfauna and flora recorded is mainly linked to the thick-skinned tectonic phase that started at the end of the Tortonian and continued to the Tortonian/Messinian boundary. This phase provoked a localized uplift, restricted even further the Rifian Corridor (Capella et al., 2017a, 2018a, b and 2019a, b) and which, locally, has

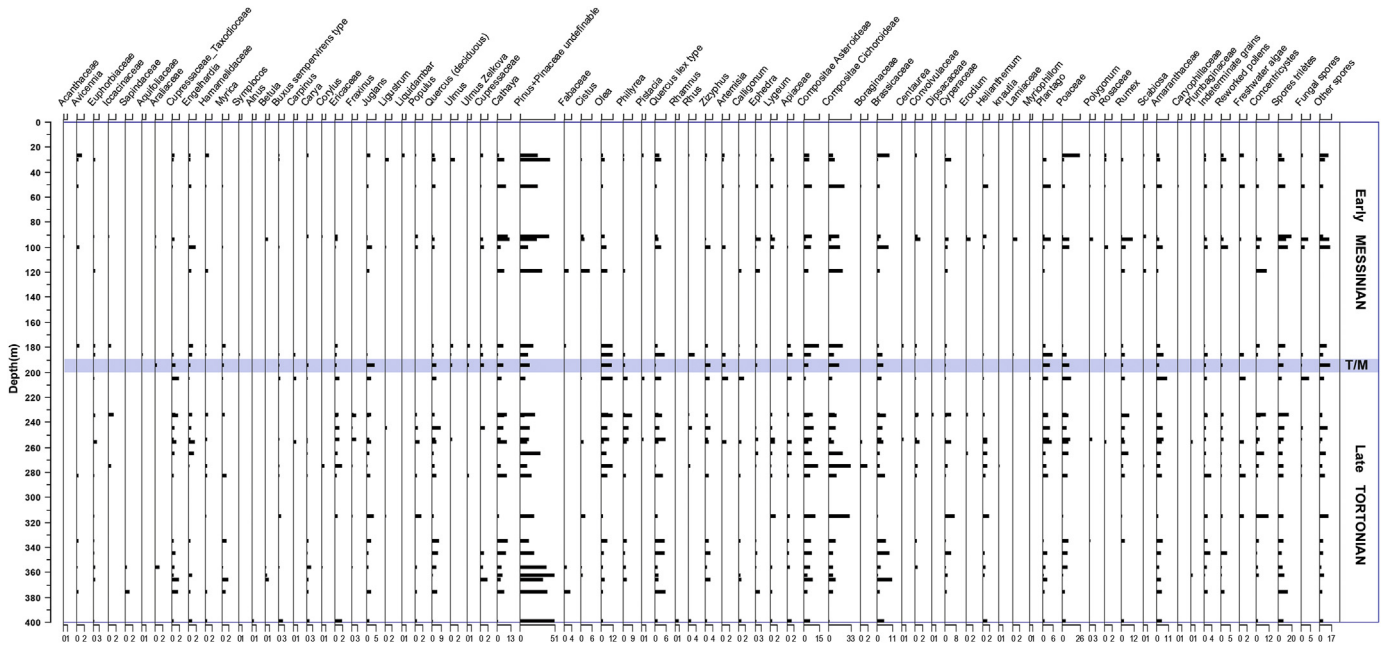

Figure 8. Detailed pollen diagram of Ain lorma1 borehole.

accentuated the glaio-eustatic drop in sea level. At Bou Regreg, the Tortonian-Messinian boundary is marked by a shift from oceanic to external platform environment (Warny et al., 2003).

The temperature index (W/C) curve has a value close to 0.8, suggesting warm sea surface conditions (Figure 10). However, from 205 to 195m, the temperature index has slightly decreased from 0.97 to 0.82. This may indicate a cooling event in sea surface water compared to the late Tortonian. Associations of planktonic foraminiferal at the same levels (205 and 195 m) reveals the dominance of *Globogerina bulloides* and *Neogloboquadrinidae* combined with a reduction or absence of *Globigerinoides obliquus*. This group of species is characteristic of cold waters (Be and Huston, 1977; Hemleben et al., 2012; Pujol and Vergnaud

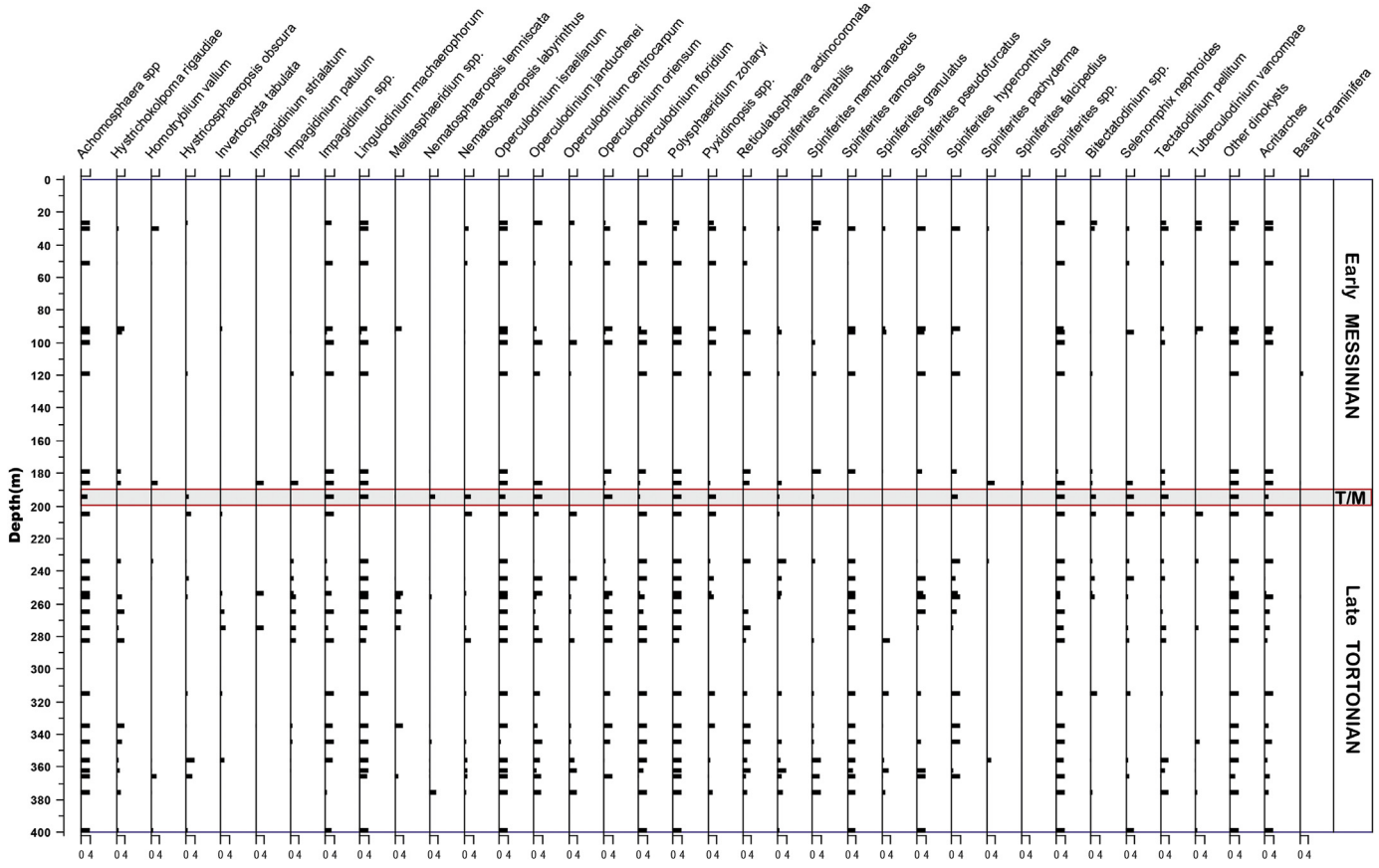

Figure 9. Detailed dinocyst diagram of Ain lorma1 borehole.

Grazzini, 1995). Also, the isotopic curve of Sale Briqueterie section in the north-west of Morocco (Hodell et al., 1994) reveals a gradual glacio-eustatic fall in sea level resulting from flow changes through the Rifian corridor as well as the onset of negative water balance in the Mediterranean Sea, due to tectonic changes in the betico-rifain corridor (Benson et al., 1991; Hodell et al., 1994, 2001; Krijgsman et al., 1999; Warny et al., 2003).

5.2.3. Early Messinian

This interval extends from 7.24 Ma to 6.51 Ma, only the deposits that characterize the lower part of this interval are present in Al-1 borehole. A single biostratigraphical event was identified there, corresponding to the influx of the *G. miotumida* (*conomiozea)* group and the abundance of *G. conomiozea* at around 161 m with an age of 7.20 to 7.18 Ma according to Lourens et al. (2004) and Sierro et al. (2001).

The P/P + B ratio varies between 50 to 60% indicating that the marine environment is open and shallow. Marine conditions persisted until 6 m.

Diversity index values are middle to high and suggest that the planktonic foraminiferal assemblages are present and diversified in some levels, while poor to rare in others. The marine environment may have been disturbed by detritic inputs.

The ratio D/S is consistently low, varying between 0.14 and 0.44. Continental inputs (pollen grains, spores, cellular organic matter and black organic matter) dominate marine inputs, it is an epicontinental environment.

Between 185 m to 100 m the distality index is above 0.5, it varies from 0.53 to 0.7, this indicates that the depositional environment remains proximal neritic (internal platform) similar to the Tortonian-Messinian transition. At 94 m the index equaled 0.5, thus confirming that proximal neritic taxa rank equally with distal ones. From 91.8 to 26.5 m the index gets lower than 0.5, along with environmental tends to be progressively more distal. The Pinaceae evolution occurs similarly to IN/ON ratio (Figure 10).

Previous works on Saïs Basin (Bachiri Taoufiq et al., 2008; Dayja et al., 2005; Capella et al., 2018a, b) also indicates a relatively deep environment (epibathyal), which corresponds to an external platform environment with tendencies towards an internal platform setting. Quite to the West (Bou Regreg), the conditions were neritic distal influenced by oceanic influences (Warny, 1999; Warny et al., 2003). At the north-eastern Morocco, in the Boudinar basin during the early Messinian the environment evolved into an open, deep marine basin with extensive tectonic (Achalhi et al., 2016).

At Early Messinian, sea level was not steady, as foraminifera and palynomorphs indicate; it evolved from a proximal to distal neritic environment. This environmental instability is caused by the regional tectonic process initiated by the indentation of the Moroccan continental margin, as a result of the mantle's resistance against the displacement of the slab towards the NNE direction (Capella et al., 2017a; 2018b). Consequently, this event has led to the closure of the Rifian corridor at around 7 Ma (Capella et al., 2017a; 2018b; 2019a; 2019b). The sea-surface temperature are warm as shown by the temperature index curve where the majority of values exceed 0, 9 (Figure 10).

5.3. Continental environments

Globally, the floristic image reflected by pollen spectra from borehole Al-1 is homogenous and evokes similar conditions from late Tortonian to the lower Messinian (Figures 8, 10).

5.3.1. Vegetal landscapes

Tortonian-Messinian microflora provided by AL-1 borehole sediments is distinguished by a combination of taxa in which the actual representatives live in intertropical regions (*Avicennia*, *Canthium* type, Euphorbiaceae, Sapindaceae, etc.), subtropical to warm-temperate zones of America and Asia (*Cathaya*, *Engelhardia*, Arecaceae, Hamamelidaceae) together with some elements actually living in Europe (deciduous

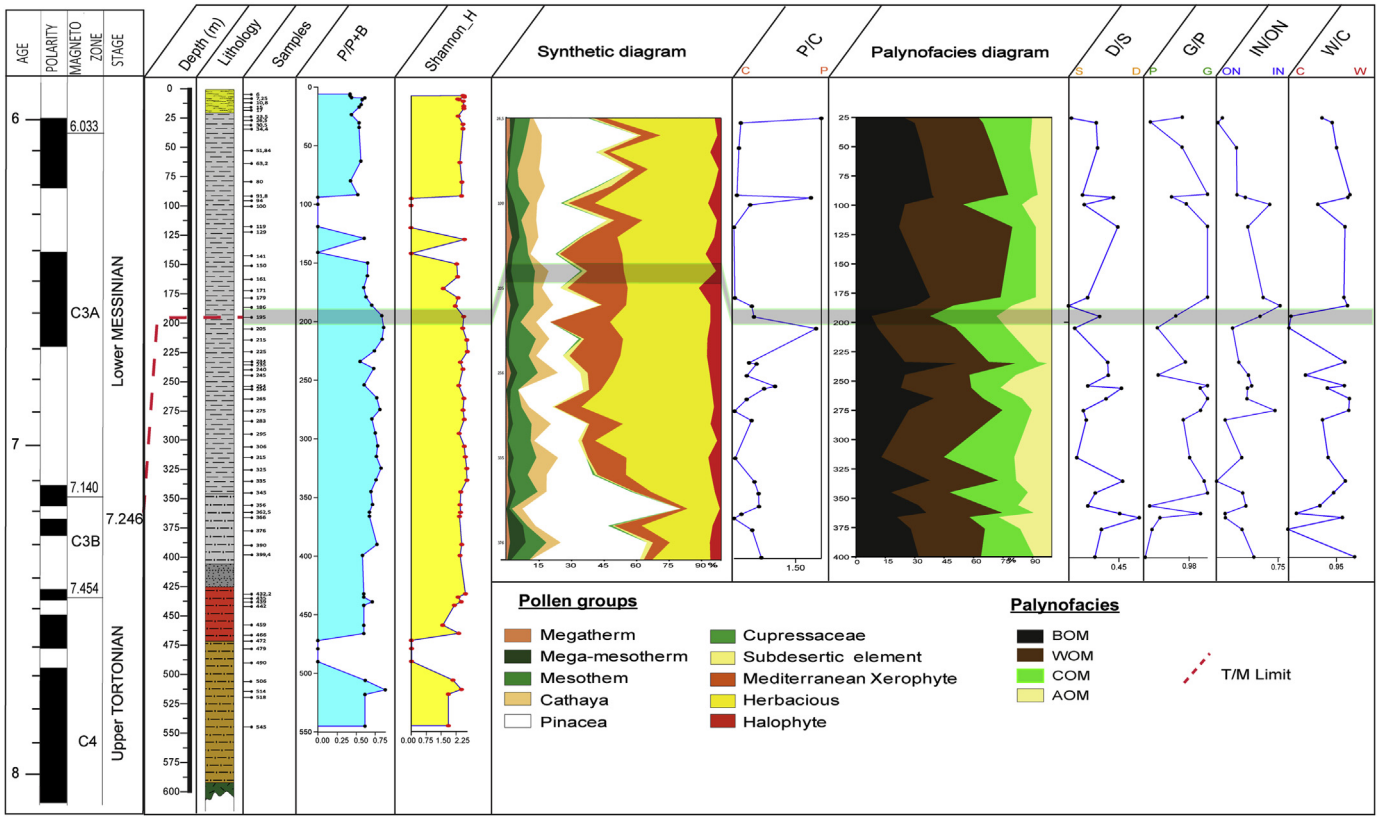

Figure 10. Quantitative results for paleoenvironmental and paleoclimatic reconstructions across Tortonian- Messinian boundary in AL-1 Borehole.

Quercus, *Ulmus*, Ericaceae, etc.) and in Mediterranean regions (*Olea*, *Ziziphus*, *Phillyrea*, *Quercus ilex-coccifera* type, *Pistacia* and *Cistus*). The representatives of sub-desert ecosystems and open vegetation cover, usually xeric (Compositae, Amaranthaceae, Plumbaginaceae, *Plantago*, *Erodium*, etc.) achieve high percentages.

In this vegetation reconstitution we will refer exclusively on elements with a known thermal and hydric exigency, acting as guide taxa, such as *Avicennia*, *Engelhardia*, *Cathaya*, *Ziziphus*, *Lygeum*, etc.

The Tortonian-Messinian coastal environment is characterized by the presence of an indicator of high thermal conditions; the *Avicennia* mangrove taxa impoverished which populated (probably discontinuously) the coast. This type of mangrove is today found between 28° and 32° North latitude, its northern extension limited by the 20 °C winter isotherm of the sea water (Hogarth, 2007). This plant now inhabits low latitude regions with tropical to subtropical climates. Its northern limit is today along the Red Sea (Kassas, 1956, 1957). The existence of this type of impoverished mangrove in the north-western Mediterranean has been documented from the lower Miocene to the middle Miocene (Bessedik, 1984, 1985; Bessedik et al., 1984), in the south-western Mediterranean (Sicily, Algeria, Morocco) up to Messinian (Suc and Bessais, 1990; Chikhi, 1992a, b; Bachiri Taoufiq., 2000, 2008). For the complete restitution of the Tortonian-Messinian coastal environment, it is also necessary to consider the presence of coral formations to which the *Avicennia* mangrove is often associated. In the terminal Miocene (on the northern edge of the Middle Atlas) coral edifices developed in the Southern Rifian corridor (Saint-Martin and Charrière, 1989; Saint-Martin and Rouchy, 1990; Bernini et al., 1992). As for the *Avicennia* mangrove, the maximum temperatures where coral reefs develop today are between 28 and 32° north latitude (Chikhi, 1992a).

In the coastal environments, the mangrove should be xerophilic and halophilic herbaceous zone including Compositae, Poaceae, Amaranthaceae, Plumbaginaceae, *Plantago*, etc. In addition, the presence of the xeric elements such as *Lygeum*, *Erodium*, *Ziziphus*, *Artemisa* and *Ephedra*, confers an arid feature to this area.

Some trees and shrubs belonging mostly to Arecaceae, Sapotaceae, Sapindaceae, Euphorbiaceae could grow in more humid places.

This open landscape must be followed in space by Mediterranean elements, consisting of *Olea*, *Ziziphus*, *Phillyrea*, *Quercusilex-coccifera* type and *Cistus*. This formation stood between an open and arboreal formation. Above the Mediterranean group develop deciduous elements (*Deciduous Quercus*, *Celtis*, *Ulmus*, *Rhus*, *Acer*, *Salix*, *Populus*, Ericaceae, *Betula*), and evergreen elements (Abietaceae, Sapotaceae, Arecaceae, and *Engelhardia*).

Around lakes and alongside rivers or on humid land, hygrophilous plants such as *Populus*, Ericaceae p. p., Sapotaceae, Arecaceae, could developed and grow. Well-drained soils were probably occupied by plants requiring less humidity (deciduous *Quecus*, *Ulmus, Betula*, *Rhus*). This mesophilous mixed forest in altitude and towards the hinterland to vegetation consisting principally of *Cathaya* and Cupressaceae in which evergreen taxa could also contribute. Pines should occupy all different vegetation layers. Rareness of high-altitude trees (*Cedrus, Abies*, *Picea*) may indicate low relief.

5.3.2. Climate

During the late Miocene, the vegetation covering the Saïs basin seems to have been singularized with several formations: an impoverished mangrove with *Avicennia*, an open low plain formation with subdesert elements, a Mediterranean element formation and a mixed mesophilic forest formation. However, the presence amongst pollen flora in coastal sediments of a mixture of dry, temperate and subtropical to tropical taxa may be explained by certain vegetation layering (Bessedik, 1985; Suc, 1986, 1989). We will attempt to deduce from this vegetation composition the climate of the Saïs basin, using the different taxa considered as being good bioclimatic indicators (see materials and methods).

The climatic reconstitution of the Saïs basin in the late Miocene, at low and mid-altitude, is as follows.

5.3.2.1. Low altitude.

We have pointed out the existence of a coral formation and a depleted mangrove with *Avicennia*, which are limited by the winter isotherm 20 °C for seawater temperature. In the Saïs basin we note that microtherm is missing, whereas megatherm, megamesotherm and mesotherm taxa are present. This lead us to estimate an annual temperature of lowlands between 20 and 24 °C, in accordance with the existence of some taxa such as *Avicennia* and *Lygeum* (Fauquette et al., 1998).

The precipitation was presumably to be very low (less than 500 mm per year). These estimates are consistent with the P/*A ratio* being less than 2 along the borehole (Figure 10). We can conclude that the lowland environments belonged to a sub-desert domain. Also, we notice that P/C ratio is less than 1, except in four levels (254m, 205m, 94m and 26.5m) where it is higher than 1. We conclude that the majority of Al-1 borehole sediments, the Compositae predominate the Poaceae, therefore the conditions were then dry in the late Tortonian and early Messinian.

5.3.2.2. Middle altitude.

The persistently high temperatures (18–21 °C) based on the presence of mega-mesothermic taxa were still to characterize the mid-altitude zone where *Engelhardia* lived, and *Cathaya*, with higher precipitation (600–700 mm).

The mean annual temperature values calculated for the sequence of Douiet in the Saïs basin using the Climatic Amplitude transfer function, gave values between 18, 4° and 24.7 °C (Fauquette et al., 2006; Suc and Fauquette, 2012) proving our estimates.

Such a warm and dry context a long time before the salinity crisis seems to confirm that the Mediterranean Sea was climatically predisposed to be desiccated when the last connecting gateway to the Atlantic Ocean closed as a consequence to tectonic activity (Warny et al., 2003; Fauquette et al., 2006; Suc et al., 2018).

5.4. Climate change during the Late Miocene and comparison with other records

During the latest Tortonian, the low altitude environments of Saïs basin must have been subject to warm and dry climatic conditions. In the marine environment the sea surface temperature is warm, as illustrated by the temperature index, which comes above 0.9 at most levels. Comparison of the temperature index curve with the SST record of Kontakiotis et al. (2019) produced for the Mediterranean reveals that at the end of the Tortonian as in the case of Sais Basin surface water conditions were very warm between (7.61–7.50 Ma). This warm climatic phase corresponds to the end of the climatic optimum developed in the Tortonian (Zachos et al., 2001 in Kontakiotis et al., 2019).

At the Tortonian-Messinian boundary, around 7.24 Ma, a major change was recognized in the Saïs Basin, consisting of an abrupt impoverishment of the marine microfauna and microflora in parallel with the increase in terrestrial inputs. The temperature index has slightly decreased (warm taxa decrease slightly as spiniferites and conversely cold taxa increase discretely), this may indicate a minor cooling in sea surface water compared to the late Tortonian. Associations of planktonic foraminiferal at the TMT reveals the dominance of cold waters species such as el que *Globogerina bulloides* and *Neogloboquadrinidae* (Be and Huston, 1977; Hemleben et al., 2012; Pujol and Grazzini, 1995). In the proximity of Gibraltar (West Alboran Sea) during TMT, open ocean sedimentation with high percentages of planktonic foraminifera typical of cold, nutrient-rich waters was recorded. This phenomena could suggest that the movement of an Atlantic inflow eastward and the eventual existence of a proto-Gibraltar Strait as the primary source of this inflow during TMT (Bulian et al., 2021). In the eastern Mediterranean the very warm interval of the late Tortonian was succeeded by a strong long-term cooling (~10 °C) and desalinization (~10‰) during the early Messinian, attributed to the paroxysmal phase of the so-called "siphon" event. This could have resulted from the restriction of the Atlantic-Mediterranean gateway under tectonic forcing, without excluding glacio-eustatic control (Kontakiotis et al., 2019). The continental environment in Saïs basin

has also registered a slight decrease in megatherms and mega-mesotherms, and an increase in Mediterranean and sub-desert elements such as *Artemisia*. This may indicate a minor decrease in temperature and increase in aridity compared to the Latest Tortonian. This reduction in temperature has also been recognized in the Italian and Iberian peninsulas (Jimenez-Moreno et al., 2010, 2013) and detected by the progressive reduction in plant diversity following the regression of thermophilic and water-intensive plants. This has been interpreted primarily as a vegetation response to global and regional processes, including climate cooling related to ice sheet development and regional mountain uplift due to the gradual movement of Eurasia and Africa (Jimenez-Moreno et al., 2010).

At the early Messinian in the Saïs basin the climatic conditions were slightly drier, for which the actual analogue is the Red Sea coast (Suc and Bessais, 1990), given the simultaneous presence of *Avicennia* (a good thermal indicator currently living in a tropical to subtropical climate) and a xerophilic herbaceous formation indicating the aridity of the environment (Compositae *Artemisia, Lygeum* .). In the marine environment, surface water conditions are warm, as shown by the temperature index curve, which has values above 0.9 in most levels (Figure 10). In the eastern Mediterranean, a significant decrease in SST (up to 10 °C) is recorded, cooling continues (7.18–6.91 Ma), with associated decrease in SSS and stress conditions for marine microfauna.

6. Conclusion

Microfauna and microflora assemblage records in the upper Miocene sediments from the Saïs Basin reflects coincident changes with the geodynamic evolution of the Rifian Corridor. A series of planktonic foraminiferal bio-events has been recorded amongst them, which has highlighted the late Tortonian and the early Messinian, and has also helped to pinpoint the Tortonian-Messinian boundary. Such events may be correlated to other Atlantic adjacent basins in the western and eastern Mediterranean.

In addition, these associations of microfauna and microflora have been used to characterize the evolution of marine and continental environments have evolved, during these periods, in a tectonically unstable area.

In the late Tortonian from 7.51 to 7.28 Ma the marine environment gets significant continental inputs. It was open, relatively deep and of an outer shelf type with occasional slight tendencies towards an inner shelf environment. These trends are explained by a remarkable tectonic control that took place between 8 and 7.25 Ma.

At the Tortonian-Messinian boundary, at about 7.24 Ma, a change was identified within the Saïs basin. The relative impoverishment of marine microfauna and microflora and the increase in terrestrial inputs could indicate a trend of the marine environment towards an internal platform environment. Moreover, the presence of cold forms within the species of planktonic foraminifera and dinokystes indicates a moderate cooling. This change is due to the rapid narrowing of the Rifian corridor at the Tortonian-Messinian boundary (Krijgsman et al., 1999) caused by tectonic phase.

In the early Messinian the marine environment corresponds to a relatively deep environment, which evolves from an internal platform environment to an external platform environment. This is due to the tectonic activity.

The predominance of warm microfaunal taxa indicates that the thermal conditions of the sea surface were warm to subtropical.

The sporopollinic contents found in sediments of Al-1 allowed reconstructing the vegetal landscape and the climate under this Mediterranean latitude. An *Avicennia* mangrove was living on the littoral and a sub-desert herbaceous cover was living at low altitude. Forests developed in middle altitude. Climate was tropical to subtropical, very dry near the coast but more humid in higher altitude. The Poaceae/Compositae rates show that aridity has even slightly increased in the Sais basin during the Late Tortonien to early Messinian. Those results confirm that climate was warm and dry a long time before the salinity Messinian crisis.

Declarations

Author contribution statement

Targhi Soukaina: Performed the experiments; Analyzed and interpreted the data; Wrote the paper.

Barhoun Nadia & Bachiri Taoufiq Naima: Conceived and designed the experiments; Analyzed and interpreted the data; Contributed reagents, materials, analysis tools or data; Wrote the paper.

Achab Mohamed: Conceived and designed the experiments.

Ait Salem Abdallah & Mohamed Zakaria Yousfi: Contributed reagents, materials, analysis tools or data.

Funding statement

This research did not receive any specific grant from funding agencies in the public, commercial, or not-for-profit sectors.

Data availability statement

Data will be made available on request.

Declaration of interests statement

The authors declare no conflict of interest.

Additional information

No additional information is available for this paper.

Acknowledgements

We would like to thank ONHYM for providing the boreholes samples and for the technical support. Many thanks addressed to the reporters who contributed by their constructive comments to improve the quality of this paper.

References

Achalhi, M., Münch, P., Cornée, J.J., Azdimousa, A., Melinte-Dobrinescu, M., Quillévéré, F., Drinia, H., Fauquette, S., Jiménez-Moreno, G., Merzeraud, G., Moussa, A.B., El Karim, Y., Feddi, N., 2016. The late Miocene Mediterranean-Atlantic connections through the north rifian corridor: new insights from the boudinar and ArbaaTaourirt basins (northeastern Rif, Morocco). Palaeogeogr. Palaeoclimatol. Palaeoecol. 459, 131–152.

Agiadi, K., Antonarakou, A., Kontakiotis, G., Kafousia, N., Moissette, P., Cornée, J.J., Manoutsoglou, E., Karakitsios, V., 2017. Connectivity controls on the late Miocene eastern Mediterranean fish fauna. Int. J. Earth Sci. 106, 1147–1159.

AitBrahim, L., Chotin, P., 1983. Mise en évidence d'un épisode compressif dans les calcaires plio-quaternaires du bassin de Saïs, Rif, Maroc. Comptes Rendus de l'Académie des Sciences de Paris 296, 1333–1336.

Antonarakou, A., Kontakiotis, G., Vasilatos, C., Besiou, E., Zarkogiannis, S., Drinia, H., Mortyn, P.G., Tsaparas, N., Makri, P., Karakitsios, V., 2019. Evaluating the effect of marine diagenesis on Late Miocene pre-evaporitic sedimentary successions of eastern Mediterranean Sea. IOP Conf. Ser. Earth Environ. Sci. 221, 12051.

Azdimousa, A., Jabaloy, A., Asebriy, L., Booth-Rea, G., Bourgois, J., Rezqui, H., AïtBrahim, L., Michard, A., Saddiqi, O., Chalouan, A., Rjimati, E., Mouttaqi, A., 2011. Rif oriental. Nouveaux Guides géologiques et miniers du Maroc/New Geological and Mining Guidebooks of Morocco, 556–564 Notes et Mémoires du Service géologique du Maroc 91–118 (2011).

Bachiri Taoufiq, N., 2000. Les environnements marins et continentaux du corridor Rifian au Miocène supérieur d'après la palynologie. PhD. thesis. université Hassan II. Casablanca, Maroc, (unpubl.).

Bachiri Taoufiq, N., Barhoun, N., Suc, J.P., 2008. Les environnements continentaux du corridor Rifian (Maroc) au Miocène supérieur d'après la palynologie. Geodiversitas 30, 41–58.

Barhoun, N., 2000. Biostratigraphie et paléo-environnement du Miocène supérieur et du Pliocène inférieur du Maroc septentrional : apport des foraminifères planctoniques. PhD thesis. Univ. Hassan II, Casablanca, Maroc (unpubl.).

Barhoun, N., Wernli, R., 1999. Biostratigraphie du Mio-Pliocène du bassin de Boudinar par les foraminifères planctoniques (Rif nord-oriental, Maroc). Rev. Paléobiol. 18, 491–508.

Bé, A.W., Hutson, W.H., 1977. Ecology of planktonic foraminifera and biogeographic patterns of life and fossil assemblages in the Indian Ocean. Micropaleontology 23 (4), 369–414.
Ben Moussa, A., Lauriat Rage, A., Piquet, J.P., 1997. Les bivalves néogènes du bassin de Saïs (Couloir sud-rifain, Maroc). In: Paléogéographie et paléoécologie. Second Congress R.C.A.N.S, Salamanca (Spain).
Benson, R.H., Rakic-El Bied, K., Bonaduce, G., 1991. An important current reversal (influx) in the Rifian Corridor (Morocco) at the Tortonian-Messinian boundary: The end of Tethys Ocean. Paleoceanography 6 (1), 165–192.
Bernini, M., Boccatelli, M., El Mokhtari, J., Iaccarino, S., Moratti, G., Papani, G., 1992. Données stratigraphiques nouvelles sur le Miocène supérieur du bassin de Taza-Guercif (Maroc nordoriental). Notes et Mémoires du service géologique du Maroc 366, 159–163.
Bessedik, M., 1984. The early aquitanian and upper Langhian-lower serravallian environments in the northwestern Mediterranean region. Paleobiol. Cont. 15 (2), 153–179.
Bessedik, M., 1985. Reconstitution des environnements miocènes des régions nord-ouest méditerranéennes à partir de la palynologie. Ph.D. thesis. USTL, Montpellier, France, p. 162.
Bessedik, M., Guin, P., Suc, J.P., 1984. Données paléofloristiques en Méditerranée nord-occidentale depuis l'Aquitanien. Revue de Paléobiologie, volume spécial 1, 25–31.
Bulian, F., Sierro, F.J., Ledesma, S., Jiménez-Espejo, F.J., Bassetti, M.A., 2021. Messinian West Alboran sea record in the proximity of Gibraltar: early signs of Atlantic-Mediterranean gateway restriction. Mar. Geol. 434.
Capella, W., Matenco, L., Dmitrieva, E., Roest, W.M., Hessels, S., Hssain, M., Chakor-Alami, A., Sierro, F.J., Krijgsman, W., 2017a. Thick-skinned tectonics closing the rifian corridor. Tectonophysics 710, 249–265.
Capella, W., Hernández-Molina, F.J., Flecker, R., Hilgen, F.J., Hssain, M., Kouwenhoven, T.J., van Oorschot, M., Sierro, F.J., Stow, D.A.V., Trabucho-Alexandre, J., Tulbure, M.A., 2017b. Sandy contourite drift in the late Miocene Rifian Corridor (Morocco): reconstruction of depositional environments in a foreland-basin seaway. Sediment. Geol. 355, 31–57.
Capella, W., Barhoun, N., Flecker, R., Hilgen, F.J., Kouwenhoven, T., Matenco, L.C., Sierro, F.J., Tulbure, M.A., Yousfi, M.Z., Krijgsman, W., 2018a. Data on lithofacies, sedimentology and palaeontology of South Rifian Corridor sections (Morocco). Data Brief 19, 712–736.
Capella, W., Barhoun, N., Flecker, R., Hilgen, F.J., Kouwenhoven, T., Matenco, L.C., Sierro, F.J., Tulbure, M.A., Yousfi, M.Z., Krijgsman, W., 2018b. Palaeogeographic evolution of the late Miocene Rifian Corridor (Morocco): reconstructions from surface and subsurface data. Earth Sci. Rev. S0012–8252(17), 30217–30219.
Capella, W., Spakman Van Hinsbergen, D.J.J., Chertova, M.V., Krijgsman, W., 2019a. Mantle resistance against Gibraltar slab dragging as a key cause of the Messinian Salinity Crisis. Terra. Nova 1–10, 2019; 00.
Capella, W., Flecker, R., Hernández-Molina, F.J., Simon, D., Meijer, P.T., Rogerson, M., Sierro, F.J., Krijgsman, W., 2019b. Mediterranean isolation preconditioning the Earth System for late Miocene climate cooling. Sci. Rep. 9, 3795.
Chalouan, A., Gil, A.J., Galindo-Zaldívar, J., Ruano, P., De Lacy, M.C., Ruiz-Armenteros, A.M., Benmakhlouf, M., Riguzzi, F., 2014. Active faulting in the frontal Rif Cordillera (Fes region, Morocco): constraints from GPS data. J. Geodyn. 77, 110–122.
Charrière, A., Saint-Martin, J.P., 1989. Relations entre les formations récifales du Miocène supérieur et la dynamique d'ouverture et de fermeture des communications marines à la bordure méridionale du sillon sud-rifain (Maroc). Comptes Rendus de l'Académie des Sciences Série II 309, 611–614.
Chikhi, H., 1992a. Une palynoflore méditerranéenne à subtropicale au Messinien pré-évaporitique en Algérie. Geol. Mediterr. 19 (1), 19–30.
Chikhi, H., 1992b. Palynoflore du Messinien infra-evaporitique de la série marno-diatomitique de Sahaouria (Beni-Chougrane) et de Chabet Bou Seter (Tessala), bassin du Chelif, Algérie. Thèse. Université d'Oran, Algérie, p. 169.
Choubert, G., Fauve Muret, A., 1962. Évolution du domaine atlasique marocain depuis les temps paléozoïques. In: Livre Mémoire P. FALLOT, Mém. H. Ser. Soc. Géol. france, 1, pp. 447–527.
CIESM, 2008. The Messinian salinity crisis from mega-deposits to microbiology. In: Briand, F. (Ed.), A Consensus Report, in 33ème CIESM Workshop Monographs, 33. CIESM, 16. bd de Suisse, MC-98000, Monaco, pp. 1–168.
Cirac, P., 1987. Le bassin sud-rifain Occidental au Néogène supérieur. Évolution de la dynamique sédimentaire et de la paléogéographie au cours d'une phase de comblement. Mem. Inst. Geol. Bassin Aquitaine 21, 1–287.
Cornée, J.J., Ferrandini, M., Saint Martin, J.P., Münch, P., Moullade, M., Ribaud-Laurenti, A., Roger, S., Saint Martin, S., Ferrandini, J., 2006. The late Messinian erosional surface and the subsequent reflooding in the Mediterranean: new insights from the Melilla– Nador basin (Morocco). Palaeogeogr. Palaeoclimatol. Palaeoecol. 230, 129–154.
Cour, P., Duzer, D., 1978. La signification climatique, édaphique et sédimentologique des rapports entre taxons en analyse pollinique. Ann. Mine. Belg. 7–8, 155–164.
Daget., J., 1979. Les modèles mathématiques en écologie. Masson, Paris.
Dayja, D., 2002. Les foraminifères néogènes, témoins de la chronologie, de la bathymétrie, et de l'hydrologie du Corridor Rifain (Maroc septentrional). Ph.D. thesis. Université P. et M. Curie (inédit).
Dayja, D., Janin, M.C., Boutakiout, M., 2005. Biochronologie et corrélation des bassins néogènes du Couloir sud-rifain (Maroc) fondées sur les évènements de foraminifères planctoniques et de nannofossiles calcaires. Rev. Micropaleontol. 48, 141–157.
Drinia, H., Antonarakou, A., Tsaparas, N., Dermitzakis, M.D., Kontakiotis, G., 2004. Foraminiferal record of environmental changes: pre-evaporitic diatomaceous sediments from Gavdos Island, southern Greece. Bull. Geol. Soc. Greece 36, 782–791.
Drinia, H., Antonarakou, A., Tsaparas, N., Kontakiotis, G., 2007. Palaeoenvironmental conditions preceding the Messinian salinity crisis: a case study from Gavdos Island. Geobios 40, 251–265.
Fassi, D., 1999. Les formations superficielles du Saïs de Fès et de Meknès. Du temps géologique à l'utilisation actuelle des sols. Notes et Mémoires du Service Géologique, Maroc 389, 527.
Fauquette, S., Quezel, P., Guiot, J., et Suc, J.P., 1998. Signification bioclimatique des taxons-guides du Pliocène méditerranéen. Geobios 31 (2), 151–169.
Fauquette, S., Suc, J.P., Bertini, A., Popescu, S.M., Warny, S., Bachiri Taoufiq, N., Perez Villa, M.J., Chikhi, H., Feddi, N., Subally, D., Clauson, G., Ferrier, J., 2006. How much did climate force the Messinian salinity crisis? Quantified climatic conditions from pollen records in the Mediterranean region. Palaeogeogr. Palaeoclimatol. Palaeoecol. 238, 281–301.
Feinberg, H., 1978. Evolution paléogéographique de l'avant-pays du Rif (Maroc) pendant le Miocène supérieur. Mémoires du Mus. Natn. Hist. Nat., Paris (518), 149–155.
Feinberg, H., Lorenz, H., 1970. Nouvelles données stratigraphiques sur le Miocène supérieur et le Pliocène du Maroc. Notes Serv. Geol. Maroc 30, 21–26.
Flecker, R., Krijgsman, W., Capella, W., De Castro Martíns, C., Demitrieva, E., Mayser, J.P., Marzocchi, A., Modestu, S., Ochoa Lozano, D., Simon, D., Tulbure, M., van den Berg, B., van der Schee, M., de Lange, G., Ellam, R., Govers, R., Gutjahr, M., Hilgen, F., Kouwenhoven, T., Lofi, J., Meijer, P., Sierro, F.J., Bachiri, N., Barboun, N., ChakorAlami, A., Chacon, B., Flores, J.A., Gregory, J., Howard, J., Lunt, D., Ochoa, M., Pancost, R., Vincent, S., Yousfi, M.Z., 2015. Evolution of the Late Miocene MediterraneanAtlantic gateways and their impact on regional and global environmental change. Earth Sci. Rev. 150, 365–392.
Frizon de Lamotte, D., Andrieux, J., Guezou, J.C., 1991. Cinématique des chevauchements néogènes dans l'Arc bético-rifain ; discussion sur les modèles géodynamiques. Bull. Soc. Geol. Fr. 162, 611–626.
Gelati, R., Moratti, G., Papani, G., 2000. The late cenozoic sedimentary succession of the Taza-Guercif basin, south rifian corridor, Morocco. Mar. Petrol. Geol. 17 (3), 373–390.
Gibson, T.G., 1989. Planktonic benthonic foraminiferal ratios: Modern patterns and Tertiary applicability. Marine. Micropaleontology 15, 29–52.
Gomez, F., Barazangi, M., Demnati, A., 2000. Structure and evolution of the Neogene Guercif basin at the junction of the middle Atlas mountains and the Rif Thrust belt, Morocco. AAPG (Am. Assoc. Pet. Geol.) Bull. 84, 1340–1364.
Gradstein, F.M., Ogg, J.G., Schmitz, M.D., Ogg, G.M. (Eds.), 2012. The Geologic Time Scale (2012). Elsevier, p. 1144.
Haq, B.U., Hardenbol, J.A.N., Vail, P.R., 1987. Chronology of fluctuating sea levels since the Triassic. Science 235 (4793), 1156–1167.
Hemleben, C., Spindler, M., Anderson, O.R., 2012. Modern Planktonic Foraminifera. Springer Science & Business Media.
Heusser, L., Balsam, W.L., 1977. Pollen distribution in the northeast Pacific ocean. Quat. Res. 7 (1), 45–62.
Hilgen, F.J., Krijgsman, W., Langereis, C.G., Lourens, L.J., Santarelli, A., Zachariasse, W.J., 1995. Extending the astronomical (polarity) time scale into the Miocene. Earth Planet Sci. Lett. 136, 495–510.
Hilgen, F.J., Krijgsman, W., Raffi, I., Turco, E., Zachariasse, W.J., 2000a. Integrated stratigraphy and astronomical calibration of the Serravallian/Tortonian boundary section at Monte Gibliscemi (Sicily, Italy). Mar. Micropaleontol. 38, 181–211.
Hilgen, F.J., Iaccarino, S., Krijgsman, W., Villa, G., Langereis, C.G., Zachariasse, W.J., 2000b. The global boundary stratotype and point (GSSP) of the Messinian stage (Uppermost Miocene). Episodes 23, 1–6.
Hilgen, F.J., Lourens, L.J., Van Dam, J.A., 2012. The Neogene period. In: Gradstein, F.M., Ogg, J.G., Schmitz, M., Ogg, G. (Eds.), The Geologic Time Scale. Elsevier, Boston, pp. 923–978.
Hodell, D.A., Benson, R.H., Kent, D.V., Boersma, A., Rakic-El Bied, K., 1994. Magnetostratigraphic, biostratigraphic, and stable isotope stratigraphy of an Upper Miocene drill core from the Sale Briqueterie (northwestern Morocco): a high-resolution chronology of the Messinian stage. Paleoceanography 9, 835–855.
Hodell, D.A., Curtis, J.H., Sierro, F.J., Raymo, M.E., 2001. Correlation of late Miocene to early Pliocene sequences between the Mediterranean and north Atlantic. Paleoceanography 16, 164–178.
Hogarth, P.J., 2007. The Biology of Mangroves and Seagrasses, second ed. Oxford University Press, New York, NY, USA, pp. 114–118. (2007).
Hsü, K.J., Ryan, W.B., Cita, M.B., 1973. Late Miocene desiccation of the Mediterranean. Nature 242 (5395), 240–244.
Iaccarino, S., 1985. Mediterranean Miocene and Pliocene planktic foraminifera. In: Bolli, H.M., Saunders, J.B., Perch-Nielsen, K. (Eds.), Plankton Stratigraphy. 1. Cambridge University Press, pp. 283–314.
Iaccarino, S., Premoli-Silva, I., Biolzi, M., Foresi, L.M., Lirer, F., Turco, E., Petrizzo, M.R., 2007. Practical manual of Neogene planktonic foraminifera. International School on Planktonic Foraminifera, 6th course. UniversitadegliStudi di Perugia.
Jimenez-Moreno, G., Fauquette, S., Suc, J.P., 2010. Miocene to Pliocene vegetation reconstructionand climate estimates in the Iberian Peninsula from pollen data. Rev. Palaeobot. Palynol. 162, 403–415.
Jiménez-Moreno, G., Pérez-Asensio, J.N., Larrasoaña, J.C., Aguirre, J., Civis, J., Rivas-Carballo, M.R., Valle-Hernández, M.F., González-Delgado, J.A., 2013. Vegetation, sea-level, and climate changes during the Messinian salinity crisis. Bull. Geol. Soc. Am. 125, 432–444.
Jolivet, L., Augier, R., Robin, C., Suc, J.P., Rouchy, J.M., 2006. Lithospheric-scale geodynamic context of the Messinian salinity crisis. Sediment. Geol. 188–189, 9–33 morel.
Karakitsios, V., Roveri, M., Lugli, S., Manzi, V., Gennari, R., Antonarakou, A., Triantaphyllou, M., Konstantina Agiadi, K., Kontakiotis, G., Kafousia *, N., Marc

de, Rafelis, 2017a. A record of the Messinian salinity crisis in the eastern Ionian tectonically active domain (Greece, eastern Mediterranean). Basin Res. 29, 203–233.
Karakitsios, V., Cornée, J.J., Tsouroua, T., Moissette, P., Kontakiotis, G., Agiadia, K., Manoutsogloud, E., Triantaphylloua, M., Koskeridoua, E., Drinia, H., Roussosa, D., 2017b. Messinian salinity crisis record under strong freshwater input in marginal, intermediate, and deep environments: the case of the North Aegean Palaeogeography. Palaeoclimatology, Palaeoecology 485, 316–335.
Kassas, M., 1956. The mist oasis of Erkwit, Sudan. J. Ecol. 44 (1), 180–194.
Kassas, M., 1957. On the ecology of the Red Sea coastal land. J. Ecol. 45 (1), 187–203.
Kili, M., 1993. Les ostracodes néogènes du sillon sud rifain (bassin du Rharb, de Saïs et de Taounate) : Paléontologie, Paleoenvironnements et Paléogeographie. PhD. thesis. Univ Rabat, p. 191.
Kontakiotis, G., Besiou, E., Antonarakou, A., Zarkogiannis, S.D., Kostis, A., Mortyn, P.G., Moissette, P., Cornée, J.-J., Schulbert, C., Drinia, H., Anastasakis, G., Karakitsios, V., 2019. Decoding sea surface and paleoclimate conditions in the eastern Mediterranean over the Tortonian-Messinian Transition. Palaeogeogr. Palaeoclimatol. Palaeoecol. 534, 109312.
Kontakiotis, G., Karakitsios, V., Cornée, J.-J., Moissette, P., Zarkogiannis, S.D., Pasadakis, N., Koskeridou, E., Manoutsoglou, E., Drinia, H., Antonarakou, A., 2020a. Preliminary results based on geochemical sedimentary constraints on the hydrocarbon potential and depositional environment of a Messinian sub-salt mixed siliciclastic-carbonate succession onshore Crete (Plouti section, eastern Mediterranean). Mediterr. Geosci. Rev. 2, 247–265.
Kontakiotis, G., Karakitsios, V., Maravelis, A.G., Zarkogiannis, S.D., Agiadi, K., Antonarakou, A., Pasadakis, N., Zelilidis, A., 2020b. Integrated isotopic and organic geochemical constraints on the depositional controls and source rock quality of the Neogene Kalamaki sedimentary successions (Zakynthos Island, Ionian Sea). Mediterr. Geosci. Rev.
Krijgsman, W., Meijer, P.T., 2008. Depositional environments of the Mediterranean "lower evaporites" of the Messinian salinity crisis: constraints from quantitative analyses. Mar. Geol. 253 (3-4), 73–81.
Krijgsman, W., Garces, M., 2004. Palaeomagnetic constraints on the geodynamic evolution of the Gibraltar Arc. Terra Nova 16 (5), 281–287.
Krijgsman, W., Hilgen, F.J., Langereis, C.G., Santarelli, A., Zachariasse, W.J., 1995. Late Miocene magnetostratigraphy, biostratigraphy and cyclostratigraphy in the Mediterranean. Earth Planet Sci. Lett. 136 (3-4), 475–494.
Krijgsman, W., Hilgen, F.J., Raffi, I., Sierro, F.J., Wilson, D.S., 1999. Chronology, causes and progression of the Messinian salinity crisis. Nature 400 (6745), 652–655.
Krijgsman, W., Hilgen, F.J., Langereis, C.G., Zachariasse, W.J., 1994. The age of the Tortonian/Messinian boundary 121, 533–547.
Krijgsman, W., Hilgen, F.J., Marabini, S., Vai, G.B., 1999a. New paleomagnetic and cyclostratigraphic age constraints on the Messinian of the Northern Apennines (Vena del Gesso Basin, Italy). Mem. Soc. Geol. It 54, 25–33.
Krijgsman, W., Langereis, C.G., Zachariasse, W.J., Boccaletti, M., Moratti, G., Gelati, R., Iaccarino, S., Papani, G., Villa, G., 1999b. Late Neogene evolution of the Taza-Guercif basin (Riffan corridor, Morocco) and implications for the Messinian salinity crisis. Mar. Geol. 153, 147–160.
Krijgsman, W., Capella, W., Simon, D., Hilgen, F.J., Kouwenhoven, T.J., Meijer, P.T., Sierro, F.J., Tulbure, M.A., van den Berg, B.C.J., van der Schee, M., Flecker, R., 2018. The Gibraltar corridor: watergate of the Messinian salinity crisis. Mar. Geol. 403, 238–246.
Lirer, F., Foresi, L.M., Iaccarino, S.M., Salvatorini, G., Turco, E., Cosentino, C., Sierro, F.J., Caruso, A., 2019. Mediterranean Neogene planktonic foraminifer biozonation andbiochronology. Earth Sci. Rev. 196, 102869 (2019).
Lourens, L., Hilgen, F.J., Laskar, J., Shackleton, N.J., Wilson, D., 2004. The Neogene period. In: Gradstein, F., Ogg, J., Smith, A. (Eds.), A Geologic Time Scale. University Press, Cambridge London, pp. 409–440.
Manzi, V., Gennari, R., Hilgen, F., Krijgsman, W., Lugli, S., Roveri, M., Sierro, F.J., 2013. Age refinement of the Messinian salinity crisis onset in the Mediterranean. Terra. Nova 25 (4), 315–322.
Margat, J., Taltasse, P., 1954. Existence d'un golfe pliocène dans la partie occidentale du couloir sud rifain (Maroc). C. r. somm. Soc. Géol. France, Paris 10, 190–193.
Martin, J., 1977. Le Moyen Atlas central. Étude Géomorphologique. PhD. thesis. Paris VI university, France.
Martin, J.M., Puga-Bernabéu, Á., Aguirre, J., Braga, J.C., 2014. Miocene Atlantic Mediterranean seaways in the betic Cordillera (southern Spain). Rev. Soc. Geol. Espana 27, 175–186.
Mathieu, R., 1986. Sédiments et foraminifères actuels de la marge continentale atlantique du Maroc. PhD. thesis. Pierre et Marie CURIE University, Paris, p. 419, 6, Paris, n° 86-14.
Mathieu, R., 1988. Foraminifères actuels et résurgences côtières sur la marge continentale atlantique du Maroc. In: Benthos'86.- Revue de Paléobiologie, pp. 845–850. Genève, vol. spécial, n° 2, Partie II.
Meijer, P.T., 2012. Hydraulic theory of sea straits applied to the onset of the Messinian Salinity Crisis. Mar. Geol. 326, 131–139.
Moissette, P., Cornée, J.J., Antonarakoua, A., Kontakiotisa, A., Driniaa, H., Koskeridoua, H., Tsouroua, H., Agiadia, H., Karakitsios, H., 2018. Palaeoenvironmental changes at the Tortonian/Messinian boundary: a deep-sea sedimentary record of the eastern Mediterranean Sea. Palaeogeogr. Palaeoclimatol. Palaeoecol. (505), 217–233.
Morel, J.L., 1988. Evolution récente de l'orogéne Rifain et de son avant pays depuis la fin de la mise en place des nappes. Mém. Géodiffusion, Paris, p. 584, 4.
Morel, J.L., 1989. Etats de contrainte et cinématique de la chaîne rifaine (Maroc) du Tortonien à l'actuel. Geodin. Acta 3, 283–294.
Morley, C.K., 1987. Origin of a major cross-element zone: Moroccan Rif. Geology 15, 761–764.
Morley, C.K., 1993. Discussion of origins of hinterland basins to the Rif-betic Cordillera and Carpathians. Tectonophysics 226, 359–376.
Murray, J.W., 1991. Ecology and Palaeoecology of Benthic Foraminifera. Longman Scientific et Technical, p. 397.
Nix, H.A., 1982. Environmental determinants of biogeography and evolution in Terra Australis. In: Barker, W.R., Greenslade, P.J.M. (Eds.), Evolution of the Flora and Fauna of Arid Australia, pp. 47–66.
Platt, J.P., Allerton, S., Kirker, A., Mandeville, C., Mayfield, A., Platzman, E.S., Rimi, A., 2003. The ultimate arc: differential displacement, oroclinal bending, and vertical axis rotation in the ExternalBetic-Rif arc. Tectonics 22 (3).
Poumot, C., Suc, J.P., 1994. Palynofaciès et dépôts séquentiels dans des sédiments marins du Néogène. Bull. Cent. Rech. Explor.-Prod. Elf-Aquitaine 18, 107–119.
Pujol, C., Grazzini, C.V., 1995. Distribution patterns of live planktic foraminifers as related to regional hydrography and productive systems of the Mediterranean Sea. Mar. Micropaleontol. 25 (2–3), 187–217.
Roveri, M., Flecker, R., Krijgsman, W., Lofi, J., Lugli, S., Manzi, V., Sierro, F.J., Bertini, A., Camerlenghi, A., De Lange, G.J., Govers, R., Hilgen, F.J., Hübscher, C., Meijer, P., Stoica, M., 2014. The Messinian Salinity Crisis: past and future of a great challenge for marine sciences. Mar. Geol. 352, 25–58.
Saint-Martin, J.P., Charrière, A., 1989. Les édifices coralliens marqueurs de l'évolution paléogéographique en bordure du Moyen Atlas (Maroc). Sci. Géologiques, Strasbourg, Mémoire 84, 83–94.
Saint-Martin, J.P., Rouchy, J.M., 1990. Les plates-formes carbonates messéniennes en Méditerranée occidentale : leur importance pour la reconstitution des variations du niveau marin au Miocène terminal. Bull. Soc. G6ol. Fr. 8, 83–94, 6, 1.
Sani, F., Zizi, M., Bally, A.W., 2000. The Neogene–Quaternary evolution of the Guercif Basin (Morocco) reconstructed from seismic line interpretation. Mar. Petrol. Geol. 17 (3), 343–357.
Sani, F., Del Ventisette, C., Montanari, D., Bendkik, A., Chenakeb, M., 2007. Structural evolution of the Rides Prerifaines (Morocco): structural and seismic interpretation and analogue modelling experiments. Int. J. Earth Sci. 96, 685–706.
Shannon, C.F., Weaver, W., 1949. The Mathematical Theory of Communication. University of Illinois Press, Urbana (Illinois), p. 322.
Sierro, F.J., 1985. The replacement of the "Globorotalia menardii" group by the "Globorotalia miotumida" group: an aid to recognizing the Tortonian-Messinian boundary in the Mediterranean and adjacent Atlantic. Mar. Micropaleontol. 9, 525–535.
Sierro, F.J., Flores, J.A., Civis, J., Gonzalez Delgado, J.A., 1987. New criteria for the correlation of the Andalusian and Messinian stages. Ann. Inst. Geol. Publ. Hung. LXX, 355–361.
Sierro, F.J., Flores, J.A., Civis, J., Gonzalez Delgado, J.A., Frances, G., 1993. Late Miocene globorotaliid event-stratigraphy and biogeography in the NE-Atlantic and Mediterranean. Mar. Micropaleontol. 21, 143–168.
Sierro, F.J., Flores, J.A., Zamarreno, I., Vazquez, A., Utrilla, R., Frances, G., Hilgen, F., Krijgsman, W., 1997. Astronomical cyclicity and sapropels in the pre-evaporitic Messinian of the Sorbas basin (Western Mediterranean). Geogaceta 21, 131–134.
Sierro, F.J., Hilgen, F.J., Krijgsman, W., Flores, J.A., 2001. The Abad composite (SE Spain): a Messinian reference section for the Mediterranean and the APTS. Palaeogeogr. Palaeoclimatol. Palaeoecol. 168, 141–169.
Simon, D., Meijer, P., 2015. Dimensions of the Atlantic–Mediterranean connection that caused the Messinian salinity crisis. Mar. Geol. 364, 53–64.
Suc, J.P., 1984. Origin and evolution of the Mediterranean vegetation and climate in Europe. Nature 307 (5950), 429–432.
Suc, J.P., 1986. Flores néogènes de méditerranée occidentale. Climat et paléogéographie. Bull. Cent. Rech. Explor.-Prod. Elf-Aquitaine 10 (2), 477–488.
Suc, J.P., 1989. Distribution latitudinale et étagement des associations végétales au Cénozoïque supérieur dans l'aire ouest-méditerranéenne. Bull. Soc. Geol. Fr. 8 (V-3), 541–550.
Suc, J.P., 1996. Late Neogene vegetation changes in Europe and north Africa. Europal Newslett 10, 27–28.
Suc, J.P., Bessais, E., 1990. Pérennité d'un climat thermo xérique en Sicile avant, pendant, après la crise de salinité messinienne. Comptes rendus de l'Académie des Sciences, série III 310, 1701–1707.
Suc, J.P., Drivaliari, A., 1991. Transport of bisaccate coniferous fossil pollen grains to coastal sediments: an example from the earliest Pliocene Orb Ria (Languedoc, Southern France). Rev. Palaeobot. Palynol. 70 (3), 247–253.
Suc, J.P., Fauquette, S., 2012. Pollen floras, a tool to estimate palaeoaltitude of mountains: the Eastern Pyrenees in the Late Neogene, a case study. Palaeogeogr. Palaeoclimatol. Palaeoecol. 321–322, 41–54.
Suc, J.P., Frizon de Lamotte, D., 2019. Paléonvironnements méditerranéens : changements et bouleversements environnementaux depuis 23 Ma. Géochronique, pp. 151–2019.
Suc, J.P., Popescu, S.M., Fauquette, S., Bessedik, M., Jiménez-Moreno, G., Bachiri Taoufiq, N., Zheng, Z., Medail, F., Klotz, S., 2018. Reconstruction of Mediterranean flora, vegetation and climate for the last 23 million years based on an extensive pollen dataset. Ecologia mediterranea, Faculté des sciences et techniques de St Jérôme, Institut méditerranéen d'écologie et de paléoécologie 44 (2), 53–85.
Suc, J.P., Saint Martin, J.P., Saint Martin, S., Popescu, S.M., Fauquette, S., 2019. Evolution des environnements marins et continentaux depuis 23 Ma dans le domaine méditerranéen. Geochronique.
Suter, G., 1980. Carte géologique de la chaine rifaine (1/500 000). Notes et mémoires N° 245a.
Taltasse, P., 1953. Recherches géologiques et hydrogéologiques dans le Bassin lacustre de Fès-Meknès. Notes et Memoires du Service Géologique du Maroc 115, 1–300.
Topper, R.P.M., Meijer, P.T., 2013. A modeling perspective on spatial and temporal variations in Messinian evaporate deposits. Mar. Geol. 336, 44–60.

Topper, R.P.M., Meijer, P.T., 2015. Changes in Mediterranean circulation and water characteristics due to restriction of the Atlantic connection: a high-resolution ocean model. Clim. Past 11 (2), 233–251.

Topper, R.P.M., Flecker, R., Meijer, P.T., Wortel, M.J.R., 2011. A box model of the late Miocene Mediterranean Sea: implications from combined 87Sr/86Sr and salinity data. Paleoceanography 26 (3).

Tulbure, M.A., Capella, W., Barhoun, N., Flores, J.A., Hilgen, F.J., Krijgsman, W., Kouwenhoven, T., Sierro, F.J., Yousfi, M.Z., 2017. Age refinement and basin evolution of the north rifian corridor (Morocco): No evidence for a marine connection during the Messinian salinity crisis. Palaeogeogr. Palaeoclimatol. Palaeoecol. 485, 416–432.

Van der Zwaan, G.J., Jorissen, F.J., de Stigter, H.C., 1990. The depth dependency of planktonic/benthic foraminiferal ratios: constraints and applications. Mar. Geol. 95, 1–16.

Van Hinsbergen, D.J.J., Kouwenhoven, T.J., Van Der Zwaan, G.J., 2005. Paleobathymetry in the backstripping procedure: correction for oxygenation effects on depth estimates. Palaeogeogr. Palaeoclimatol. Palaeoecol. 221 (3), 245–265.

Van Hinsbergen, D.J.J., Vissers, R.L.M., Spakman, W., 2014. Origin and consequences of western Mediterranean subduction, rollback, and slab segmentation. Tectonics 33, 393–419.

Vasiliev, I., Karakitsios, V., Bouloubassi, I., Agiadi, K., Kontakiotis, G., Antonarakou, A., Triantaphyllou, M., Gogou, A., Kafousia, N., de Rafélis, M., Zarkogiannis, S., Kaczmar, F., Parinos, C., Pasadakis, N., 2019. Large sea surface temperature, salinity, and productivity-preservation changes preceding the onset of the Messinian Salinity Crisis in the eastern Mediterranean Sea. Paleoceanogr. Paleocl.

Vasiliev, I., Reichart, G.-J., Krijgsman, W., 2013. Impact of the Messinian Salinity Crisis on Black Sea hydrology—Insights from hydrogen isotopes analysis on biomarkers. Earth Planet. Sci. Lett. 362, 272–282.

Vergés, J., Fernàndez, M., 2012. Tethys-atlantic interaction along the Iberia-Africa plate boundary: the betic-Rif orogenic system. Tectonophysics 579, 144–172.

Warny, S., 1999. Mio-pliocene Palynology of the Gibraltar Arc: a New Perspective on the Messinian Salinity Crisis. PhD. Thesis. Université Catholique de Louvain, Faculté des Sciences, p. 305.

Warny, S., Bart, P.J., Suc, J.-P., 2003. Timing and progression of climatic, tectonic and glacioeustatic influences on the Messinian Salinity Crisis. Palaeogeogr. Palaeoclimatol. Palaeoecol. 202, 59–66.

Wernli, R., 1988. Micropaléontologie du Néogène post-nappes du Maroc septentrional et description systématique des foraminifères planctoniques. Notes et Mém. Serv. géol. Maroc 331, 270.

Zachos, J.C., Shackleton, N.J., Revenaugh, J.S., Pälike, H., Flower, B.P., 2001. Climate response to orbital forcing across the Oligocene-Miocene boundary. Science 292 (5515), 274–278.

Zizi, M., 1996. Triassic–Jurassic extension and Alpine inversion in the northern Morocco. In: Ziegler, P.A., Horvath, F. (Eds.), Peri-Tethys Memoir 2: Structure and Prospects of the Alpine Basins and Forelands. Mémoires du Muséum National d'Histoire Naturelle, 170, pp. 87–101. Paris.